



**MARINET**

*Marine Renewables Infrastructure Network*

Work Package 4: Research

# D4.06 Data Reports and Databases: Data on coastal and offshore wind measurements

Author(s):

Mike Courtney	DTU
Alfredo Peña	DTU
Rozenn Wagner	DTU
Johan Peeringa	ECNETH
Arno Brand	ECNETH
Julia Gottschall	FH-IWES
Andreas Rettenmeier	USTUTT
Fabio Pierella	NTNU



Revision: 03  
Date: 21-Feb-2014































## ABOUT MARINET

MARINET (Marine Renewables Infrastructure Network for Emerging Energy Technologies) is an EC-funded consortium of 29 partners bringing together a network of 42 specialist marine renewable energy testing facilities. MARINET offers periods of free access to these facilities at no cost to research groups and companies. The network also conducts coordinated research to improve testing capabilities, implements common testing standards and provides training and networking opportunities in order to enhance expertise in the industry. The aim of the MARINET initiative is to accelerate the development of marine renewable energy technology.

Companies and research groups who are interested in availing of access to test facilities free of charge can avail of a range of infrastructures to test devices at any scale in areas such as wave energy, tidal energy and offshore-wind energy or to conduct specific tests on cross-cutting areas such as power take-off systems, grid integration, moorings and environmental data. In total, over 700 weeks of access is available to an estimated 300 projects and 800 external users.

MARINET consists of five main areas of focus or 'Work Packages': Management & Administration, Standardisation & Best Practice, Transnational Access & Networking, Research and Training & Dissemination. The initiative runs for four years until 2015.

## Partners

  	<p><b>Ireland</b>            University College Cork, HMRC (UCC_HMRC)  <i>Coordinator</i>            Sustainable Energy Authority of Ireland (SEAI_OEDU)</p>	<p><b>Netherlands</b>            Stichting Tidal Testing Centre (TTC)            Stichting Energieonderzoek Centrum Nederland (ECNeth)</p>	 
	<p><b>Denmark</b>            Aalborg Universitet (AAU)            Danmarks Tekniske Universitet (RISOE)</p>	<p><b>Germany</b>            Fraunhofer-Gesellschaft Zur Foerderung Der Angewandten Forschung E.V (Fh_IWES)            Gottfried Wilhelm Leibniz Universität Hannover (LUH)            Universität Stuttgart (USTUTT)</p>	  
 	<p><b>France</b>            Ecole Centrale de Nantes (ECN)            Institut Français de Recherche Pour l'Exploitation de la Mer (IFREMER)</p>	<p><b>Portugal</b>            Wave Energy Centre – Centro de Energia das Ondas (WavEC)</p>	
      	<p><b>United Kingdom</b>            National Renewable Energy Centre Ltd. (NAREC)            The University of Exeter (UNEXE)            European Marine Energy Centre Ltd. (EMEC)            University of Strathclyde (UNI_STRATH)            The University of Edinburgh (UEDIN)            Queen's University Belfast (QUB)            Plymouth University (PU)</p>	<p><b>Italy</b>            Università degli Studi di Firenze (UNIFI-CRIACIV)            Università degli Studi di Firenze (UNIFI-PIN)            Università degli Studi della Tuscia (UNI_TUS)            Consiglio Nazionale delle Ricerche (CNR-INSEAN)</p>	   
 	<p><b>Spain</b>            Ente Vasco de la Energía (EVE)            Tecnalia Research &amp; Innovation Foundation (TECNALIA)</p>	<p><b>Norway</b>            Sintef Energi AS (SINTEF)            Norges Teknisk-Naturvitenskapelige Universitet (NTNU)</p>	 
	<p><b>Belgium</b>            1-Tech (1_TECH)</p>		

## Acknowledgements

The research leading to these results has received funding from the European Union Seventh Framework Programme (FP7) under grant agreement no. 262552.

## Legal Disclaimer

The views expressed, and responsibility for the content of this publication, lie solely with the authors. The European Commission is not liable for any use that may be made of the information contained herein.

## REVISION HISTORY

Rev.	Date	Description	Author	Reviewed by
01	6 November 2013	First Draft	Fabio Pierella	
02	29 November 2013	Sector-scanning and Intro chapters added.	Mike Courtney	Jochen Giebhardt
03	21 Feb. 14	Revised data for the sector scanning chapter. Some editing of figures. Conclusion (section 4) added. References enumerated.	Mike Courtney	Rozenn Wagner



## EXECUTIVE SUMMARY

This report is the contractual deliverable for Marinet work task 4.3.1. This document consists of an introduction (Section 1) to the work and reporting of task 4.3. A survey of existing wind datasets is given in Section 2. In Section 3 an experiment to examine the feasibility of using coastally positioned scanning lidars to measure the near-shore wind resource. Overall conclusions are given in Section 4.



# CONTENTS

<b>1</b>	<b>INTRODUCTION .....</b>	<b>6</b>
<b>2</b>	<b>EXISTING OFFSHORE WIND DATA SETS .....</b>	<b>7</b>
2.1	THE VINDEBY WIND FARM EXPERIMENT (2001).....	7
2.1.1	<i>Objectives, setup, and instrumentation .....</i>	<i>7</i>
2.1.2	<i>General results .....</i>	<i>8</i>
2.2	THE NYSTED WIND FARM EXPERIMENT (2005).....	9
2.2.1	<i>Setup and instrumentation.....</i>	<i>9</i>
2.2.2	<i>Objectives, issues and general results.....</i>	<i>9</i>
2.3	ZEPHIR AT FINO1 (2006).....	10
2.3.1	<i>Objectives, setup and instrumentation .....</i>	<i>10</i>
2.3.2	<i>Results .....</i>	<i>11</i>
2.4	THE 12 MW PROJECT (2006).....	11
2.4.1	<i>Objectives, setup and instrumentation .....</i>	<i>11</i>
2.4.2	<i>Results .....</i>	<i>12</i>
2.5	NORSEWIND PROJECT (2008).....	14
2.5.1	<i>Objectives, setup and instrumentation .....</i>	<i>14</i>
2.5.2	<i>Results .....</i>	<i>14</i>
2.6	WINDCUBE AT FINO1 (2009) .....	16
2.6.1	<i>Objectives, setup and instrumentation .....</i>	<i>16</i>
2.6.2	<i>Results .....</i>	<i>16</i>
2.7	ZEPHIR AT FINO3 (2011).....	17
2.7.1	<i>Objectives, setup and instrumentation .....</i>	<i>17</i>
2.7.2	<i>Results .....</i>	<i>18</i>
2.8	TALL WIND PROFILE OFFSHORE EXPERIMENT (2013).....	19
2.8.1	<i>Objectives, setup and instrumentation .....</i>	<i>19</i>
2.8.2	<i>Results .....</i>	<i>19</i>
<b>3</b>	<b>SCANNING LIDAR MEASUREMENTS FROM COASTAL SITES .....</b>	<b>21</b>
3.1	INTRODUCTION .....	21
3.2	TEST SITE AND INSTRUMENTATION.....	23
3.3	THE TEST SETUP .....	25
3.3.1	<i>Leveling the lidar .....</i>	<i>27</i>
3.3.2	<i>Verification of the lidar azimuth angle indication.....</i>	<i>28</i>
3.3.3	<i>Verification of the lidar scanner head elevation angle .....</i>	<i>29</i>
3.3.4	<i>Met mast azimuth and elevation angles.....</i>	<i>29</i>
3.4	RESULTS.....	29
3.4.1	<i>Verification of the consistency of the beam orientation .....</i>	<i>29</i>
3.4.2	<i>Radial wind speed measurement .....</i>	<i>34</i>
3.4.3	<i>Sector scanning results.....</i>	<i>36</i>
3.5	SECTOR-SCANNING RESULTS – DISCUSSION .....	39
<b>4</b>	<b>CONCLUSIONS .....</b>	<b>40</b>
	<b>REFERENCES .....</b>	<b>41</b>

# 1 INTRODUCTION

Offshore wind power is an important marine renewable energy. Determining and characterising the wind offshore is a demanding challenge largely because wind measurements are so sparse. The Marinet project has a work task (4.3) devoted to marine wind measurements and this documents represent the contractual deliverable of that task. Work task 4.3 has undertaken three main pieces of work:

Firstly a thorough survey of offshore wind measuring techniques has been made including an analysis of how well these technologies are covered by existing standards and best practice documents. Some considerable attention is paid to the application of lidars, both on fixed and floating platforms, since lidars have the potential to provide wind measurements where other technologies, notably traditional masts, cannot. This work is reported in Deliverable D4.16.

Secondly a survey of existing wind data sets has been made since much good research material is already available. Experiments listed range from those at the world's first offshore wind farm Vindeby in 2001 to a contemporary experiment aimed at examining the nature of tall wind profiles. This work is reported in Section 2 of this document.

Lastly we have chosen to perform an experiment with a promising technique for measuring the wind in near-shore waters. Lidars have developed in power and accuracy to the point where they can be placed on-land and perform measurements over the water, to ranges of about 10km. An experiment to simulate such measurements has been performed on-land. This is reported in Section 3 of this document.

## 2 EXISTING OFFSHORE WIND DATA SETS

Here we provide a brief overview of some of the existing offshore wind datasets focused on observations performed with remote sensors (RSs), such as wind lidars, sodars, and ceilometers. This overview does not take into account floating and buoy RSs deployments. The authors are aware of other existing offshore campaigns using RSs but the data and the results of such campaigns are either confidential, under current analysis, or beyond the knowledge of them. Among those campaigns:

- Naikun, Hecate Strait (2006): ZephIR wind lidar (<http://www.zephirlidar.com/project-timeline/offshore>)
- Cleveland Crib, Great Lakes (2009): ZephIR wind lidar (see above webpage)
- Robin Rigg, Solway Firth (2010): ZephIR wind lidar (see above webpage)
- Dogger Bank, North Sea (2011) : ZephIR wind lidar (see above webpage)
- Fino1, North Sea (2012): Galion wind scanning lidar (<http://www.sgurrenergy.com/first-3d-scanning-lidar-deployed-on-fino1/>)
- Fino2, Baltic Sea (2012): WindCube v1 and v2 wind lidars ([http://www.dnv.pl/Binaries/4%20Offshore%20Met%20Mast%20Planning,%20Risk%20and%20Design%20-%20Detlef%20Stein\\_tcm144-533935.pdf](http://www.dnv.pl/Binaries/4%20Offshore%20Met%20Mast%20Planning,%20Risk%20and%20Design%20-%20Detlef%20Stein_tcm144-533935.pdf))
- Great Lakes 3D wind experiment (2012): ZephIR and Galion wind lidars (<http://geology.indiana.edu/barthelmie/windFarm/index.html>)
- High resolution Doppler lidar (HRDL) and Master-Oscillator/Power-Amplifier (MOPA) systems used in a number of offshore experiments (see details in Pichugina et al., [22])
- Alpha Ventus and Fino1, North Sea (2012) (see details in Cañadillas and Neumann., [4])
- Alpha Ventus, North Sea (2012): WindCube wind lidars (see details in the Chapter by Rettenmeier et al. in Peña et al., [16])

### 2.1 THE VINDEBY WIND FARM EXPERIMENT (2001)

#### 2.1.1 Objectives, setup, and instrumentation

One of the first experiments using RSs offshore was performed at the Vindeby wind farm in Denmark using a ship-mounted mini-sodar (AV4000 from AeroVironment). The purpose was to measure wind turbine wakes (magnitude and vertical extent), evaluate the utility of sodar to measure offshore wind profiles, and provide the first offshore wake measurements with varying distances from the turbine (see Figure 1). Details about the experiment and observations can be found in [2] and [3].

Hub height of the wind turbines is 38 m and rotor diameter (D) of 35.5 m. The sodar was mounted on a highly stable (in terms of tilt and position) ship. Three wake distances over a distance of 150—200 m were used. The sodar's first three range gates (15, 20 and 25 m) were excluded due to poor number of returns; a height resolution of 5 m with a maximum range of 200 m was used. The mast data provided measurements of wind speed and direction within the range 10—47.5 m AMSL.

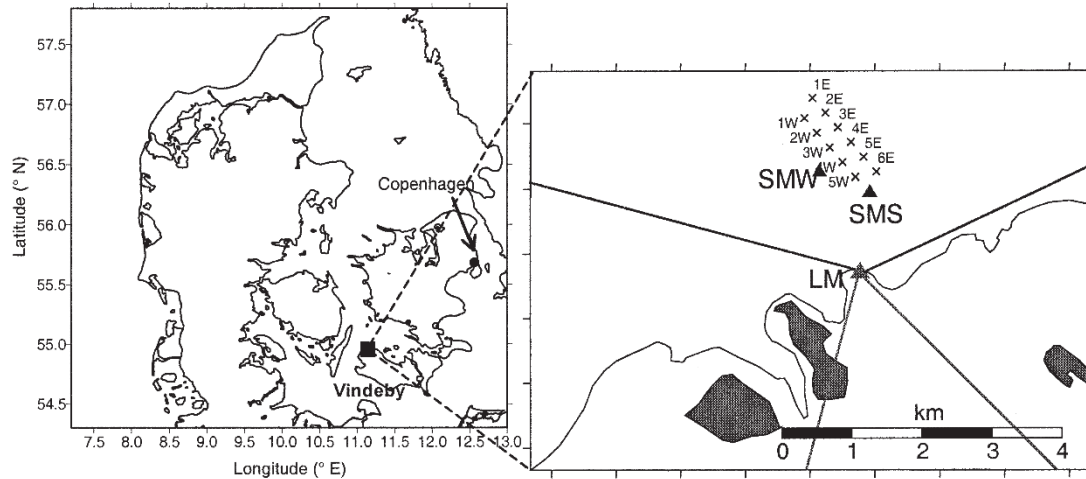


Figure 1 Layout of the Vindeby wind farm in Denmark. SMW, SMS and LM are reference masts (from Barthelmie et al., [3])

## 2.1.2 General results

Specific experiments (36 in total) were carried out at Vindeby; among them a free stream and one wake measurement, a one wake turbine-on turbine-off measurement, and single wake experiments. Results from these experiments were compared with wake predictions using an empirical model for the wind speed deficit. Figure 2 shows a comparison of the sodar wind speed profile with those observed from two of the masts for free and wake conditions (wind direction was steady and always about 340°). The free sodar profile was measured when the sodar was positioned besides SMW. Then when moved close to turbine 1W, it measured the single wake of the turbine.

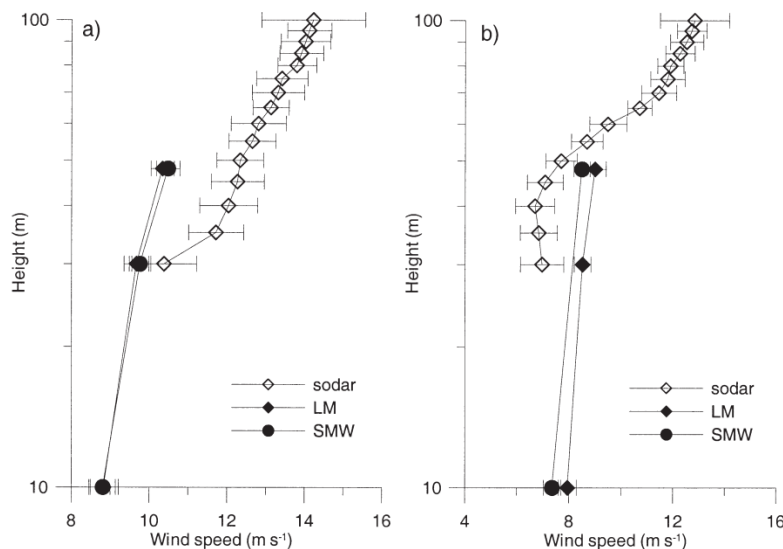


Figure 2 Free-stream (left) and wake (right) wind speed profiles measured by the masts and the sodar at Vindeby (from Barthelmie et al., [3])

For this particular experiment, there was good agreement between the sodar and the mast measurements at 30 m but large differences at 48 m (for the free profile on the left frame) revealing a high degree of uncertainty about the sodar observations. Generally, the sodar operated well and showed wind speed deficit, as expected, from the wakes of the turbines.



## 2.2 THE NYSTED WIND FARM EXPERIMENT (2005)

### 2.2.1 Setup and instrumentation

Two sodars (an AQ500 wind profiler from AQ systems and an AV4000) and a wind lidar (a Zephir prototype from QinetiQ) were mounted on top of a 20-m offshore transformer/platform close to the Nysted wind farm. The transformer is located 200 m north of the fifth north-south row of turbines of the wind farm (see Figure 3). Observations with the three RSs were carried out over a period of two months.

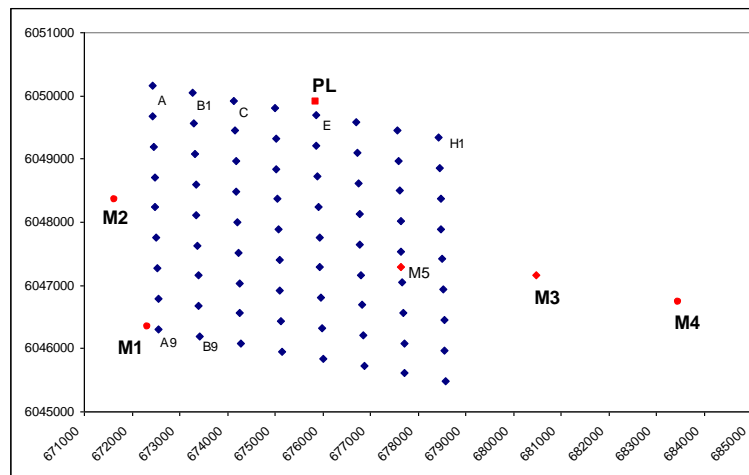


Figure 3 The Nysted wind farm experiment showing the layout of the turbines, the masts (M1-M5), and the platform (PL) location (from Antoniou et al., [1])

### 2.2.2 Objectives, issues and general results

As this was one of the first campaigns where such RSs were deployed offshore, the first objective was to evaluate whether the instruments could operate for such an extended operation period. The second was to observe the influence of the wind farm on the atmospheric boundary layer (ABL). The instruments operated rather well; wind profiles were obtained above the turbine's blade tip height (110 m) and were consistent with those measured by the met masts.

The instruments operated during a period of high temperature and the cooling systems were therefore working at full capacity. This increased the background noise deteriorating the signal of the two sodars and thus their availability. The three instruments were working in a wind profile mode; therefore the availability of the sodar signal deteriorated with height and so measurements didn't all the time reached the maximum sampling altitude (200 and 400 m for the AV4000 and the AQ500, respectively). The wind lidar was measuring at five heights up to a height of approx. 155 m above mean sea level (AMSL).

Figure 4 illustrates the mean wind speed profiles measured by the RSs at Nysted for concurrent measurements at all common heights for all sectors. Wind profiles from the AQ500 and the wind lidar are similar and those of the AV4000 differ the most. Antoniou et al. [1] argued that the differences for this sodar are due to fixed echoes observed at the first measurement height.

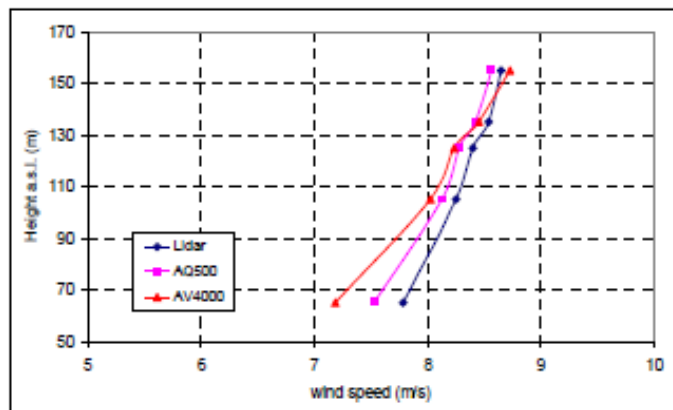


Figure 4 The mean wind speed profiles measured by the three RSs from concurrent measurements at common heights (from Antoniou et al., [1])

The profiles were further classified into different stability conditions based on free wind speed conditions and the mast observations. Wake and non-wake influenced profiles were also studied. Figure 5 shows some of the observed free wind stream profiles from combining met mast measurements with the different RSs. The agreement is fairly good but it is already seen that the mast measurements were distorted by the mast itself and, thus, mast profiles appear less “logarithmic” than those retrieve with the RSs.

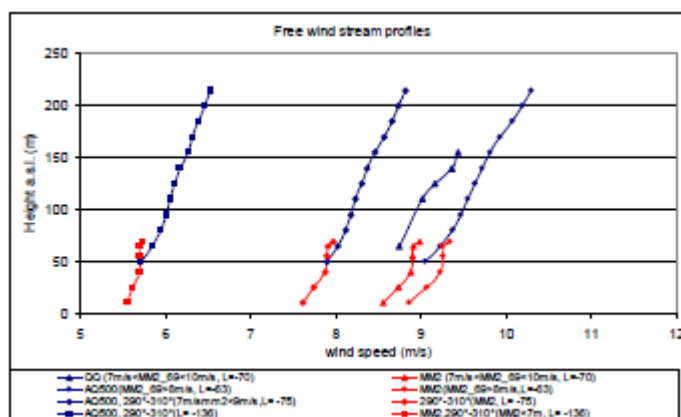


Figure 5 The free wind speed profiles from combined RSs with the mast measurements (from Antoniou et al., [1])

Although the agreement of the wake-influenced profiles is not as good as that for the free sectors, the wake was observed to exceed the measured heights. The main objective of the campaign, which was to observe the suitability of RSs for offshore measurements, was covered by the results of the experiment.

## 2.3 ZEPHIR AT FINO1 (2006)

### 2.3.1 Objectives, setup and instrumentation

From March to July 2006, the first commercial available wind lidar (QinetiQ’s ZephIR) was installed at the Fino1 offshore research platform in the German Bight area of the North Sea, 45 km north of the island of Borkum. The instrument was placed 25 m AMSL and during a one month period it measured winds at 103 m (to be compared with the highest cup at the mast) and during the rest of the campaign scanned conically the vertical wind profile at 61, 81, 103, and 125 m AMSL. The mast is equipped with cup and sonic anemometers and other instrumentation at several levels (see details in [11]) and overlapped the wind lidar observations at 61, 81, and 103 AMSL. The main objective of the campaign was to investigate the performance and capabilities of the ZephIR system and to study the its suitability for being the primary wind data source on the Beatrice project.

## 2.3.2 Results

Main results of the experimental campaign were related to the validation of the wind lidar observations with the cup anemometer measurements at the mast. Figure 6 illustrates the scatter plot observed at the highest height at Fino1, where both mast and wind lidar overlapped. Generally, very good correlation was found for the wind speed observations with a slight decrease with height (the results for the other heights are not shown). An overall wind lidar data availability of 98% was achieved.

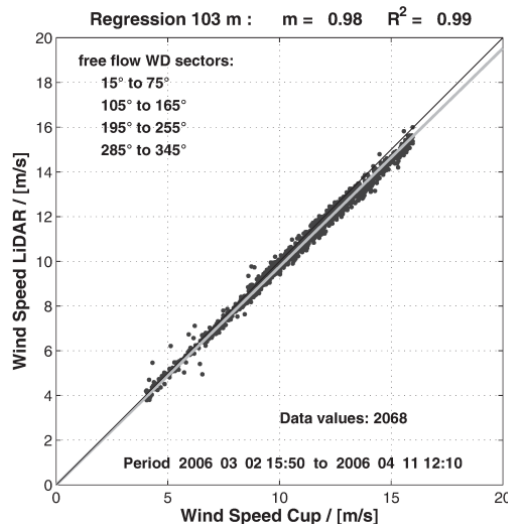


Figure 6 Scatter plot of the 10-min horizontal wind speed measured by the cup anemometer and the wind lidar at the overlapping height of 103 m at Fino1 (from Kindler et al., [11])

One of the interesting results of the campaign was related to the influence of clouds in the ZephIR measurements. The cloud correction algorithm resulted in better correlations as found without it. Also interesting is that the wind lidar measurements “intersected” the mast but this didn’t seem to cause a reduction of the correlation of wind speed measurements.

## 2.4 THE 12 MW PROJECT (2006)

### 2.4.1 Objectives, setup and instrumentation

The 12 MW project aimed to investigate the wind conditions in which possible 12 MW/very large wind turbines were to operate and to establish the scientific basis relevant for the next generation of large offshore wind turbines. A six month experimental campaign (May to October 2006) was therefore carried out at the Horns Rev I wind farm located in the Danish North Sea 12–17 km from the west coast of Jutland, Denmark (see Figure 7). The project was developed between the former Risø National Laboratory (now DTU Wind Energy) and DONG Energy.

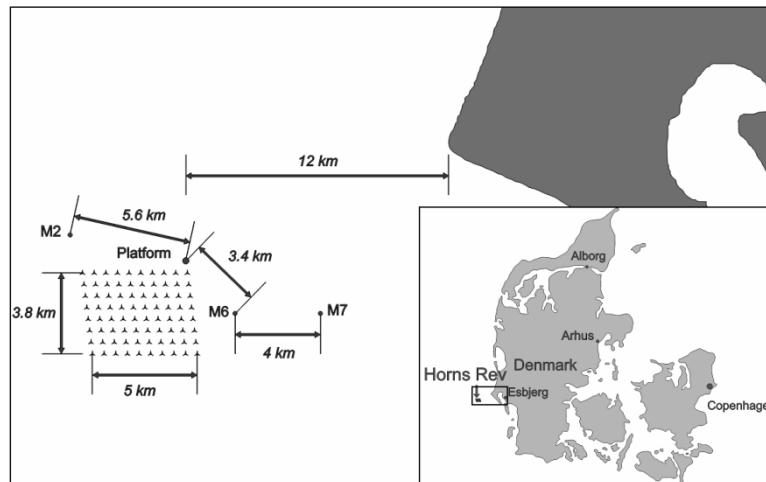


**Figure 7: Layout of the Horns Rev wind farm in the Danish North Sea (from Peña et al., [20])**

Three met masts performed observations of wind and sea conditions from 4 m below mean sea level (BMSL) to about 62/70 m AMSL (M2, M6 and M7). These were complemented by measurements from RSs installed on the deck of the transformer/platform of the wind farm at the north-east corner: a wind lidar (QinetiQ's ZephIR) measuring at 5 different heights up to 161 m AMSL and a sodar (AQ500).

## 2.4.2 Results

The project is described in detail in [9] and several papers and conference proceedings contain results obtained from the analysis of the measurements from 12 MW. Here we focused on those reported in some of the peer-reviewed journals. The work was focused on the free stream conditions, as wake conditions are very difficult to characterize based on the lidar measurements at the platform of the wind farm.

Peña et al. [20] showed basic results from the 12 MW campaign. There the wind lidar measurements are the basis of the study as the AQ500 sodar did not perform well due to possible noise contamination from bird alarms (to prevent accidents from landing helicopters to the platform), fixed echoes (from the nearby platform crane), and background noise (from the sea and operation units).

In the analysis, the spectra scaling factor was used for the first time to discriminate possible cloud contamination of the measurements (procedure later refined and adapted by QinetiQ). As this was a continuous wave (CW) lidar, the measurements were hardly influenced by the backscatter from clouds since the measurement volumes largely increase with height.

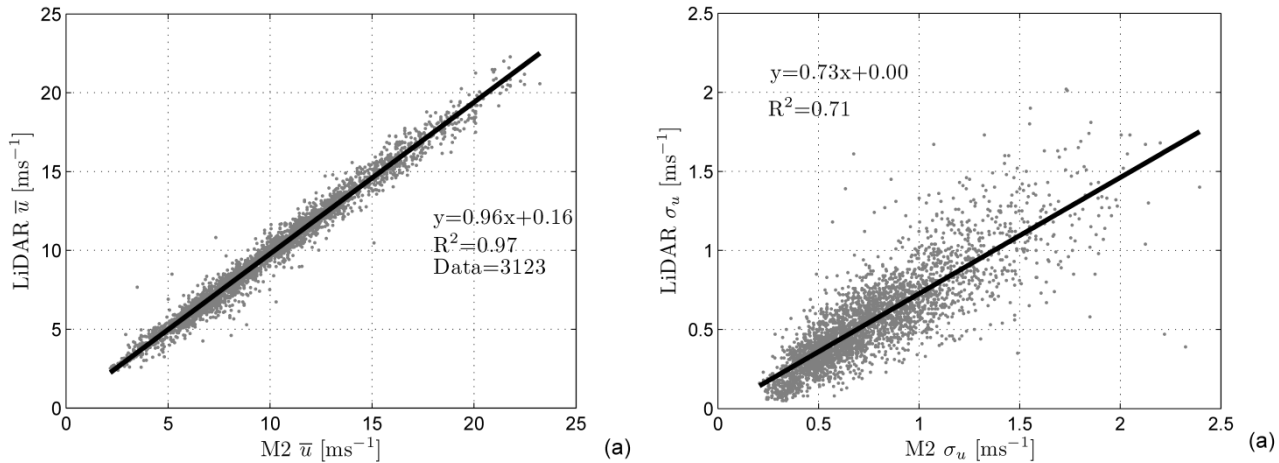


Figure 8: Comparison of horizontal wind speeds (left) and standard deviations (right) from the wind lidar at 63 m against the cup anemometer at 62 m at M2 (from Peña et al., [20])

Mean wind speeds and turbulence quantities were compared between the wind lidar on the platform and the different masts. Figure 8 illustrates such comparisons, where good agreement and correlation was found for the mean wind speed, whereas the agreement deteriorates for the standard deviation. Wind lidar turbulence measurements and modelling were also studied from this dataset later on by Mann et al. [12].

Already in Peña et al. [20] the influence of the variable sea surface roughness was analysed and the study of Peña and Gryning [14] based on M2 data of both wind speed and atmospheric stability measures came up with a methodology for the analysis of offshore wind speed profiles. This was later implemented in the work by Peña et al. [19], who provided wind speed profile parameterizations for offshore winds covering the whole boundary layer, so they are boundary-layer height (BLH) dependent.

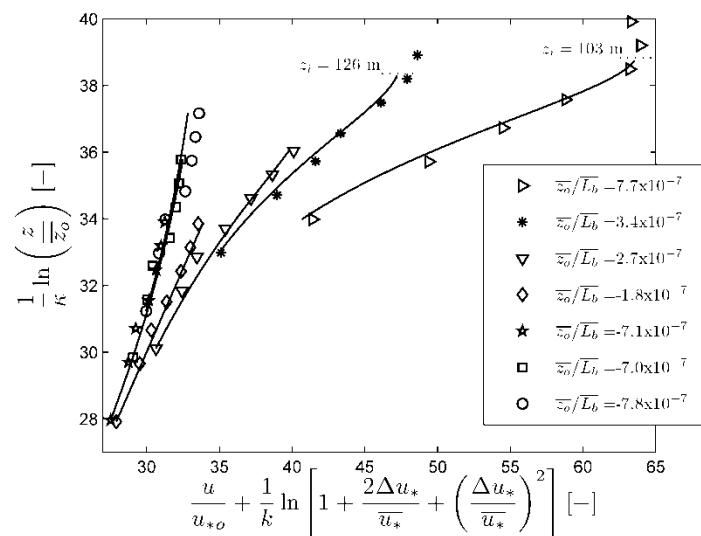


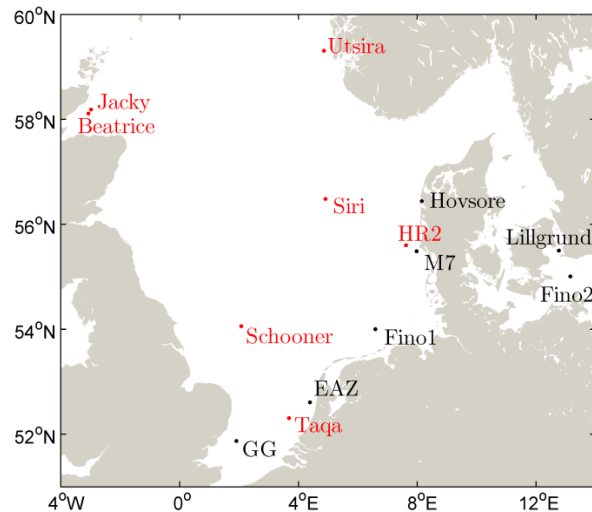
Figure 9: Non-dimensional wind speed profiles from measurements (markers) and the expressions taking into account the BLH (solid lines) for different atmospheric stability classes (from Peña et al., [19])

Figure 9 shows the main results of the latter study in which the wind speed profiles are displayed using a non-dimensional form for different stability classes from the combined M2 and wind lidar measurements (from 15 up to 161 m AMSL). The expressions including the BLH showed much better agreement with the measurements under stable conditions than the traditional diabatic wind speed profiles derived from Monin-Obukhov similarity theory.

## 2.5 NORSEWIND PROJECT (2008)

### 2.5.1 Objectives, setup and instrumentation

The Northern Seas Wind Index database project, also known as NORSEWIND, had the main purpose of observing the wind regime in the Northern European seas by means of setting up a network of mast measurements and RSs installed on transformers, platforms, and oil and gas rigs (see Figure 10). Main objectives of the measurement campaign were to analyse the observations of the vertical wind shear and the effects of the platforms, rigs and structures on the wind flow observed by the RSs.



**Figure 10: Meteorological and wind lidar stations of the NORSEWIND project (from Peña et al., [21])**

In total there were 7 wind lidars installed along the Northern Seas (some other were also used as part of the project but were later incorporated into the main project's database), from which six are pulsed wind lidars (WindCube v1 and v2 types) and one CW wind lidar (a ZephIR). The lidars were installed at locations where there were no measurements from masts. Therefore, on-site validation of the measurements was not possible and so some of the instruments were validated against the met mast at Høvsøre prior and after the operational period. Also, due to the lack of mast measurements at the wind lidar deployments, no direct measurements of atmospheric stability were possible. This restricted the use of the wind lidar observations for analysing the vertical wind shear at turbine's operating heights, as one of the major contributors to the behaviour of the wind speed profile is atmospheric stability. Generally, the wind lidars performed well and observed winds from a height of about 60 to 300 m AMSL. Details about the observations and the results are given in Peña et al. [21].

### 2.5.2 Results

Different type of results resulted from the analysis of the observations from the NORSEWIND lidars. For all the wind lidar nodes, the wind profiles were analysed to see the effect of fetch and wakes for different wind sectors. Figure 11 illustrates the mean wind speed profiles measured in each of the 12 sectors by the wind lidar at Horns Rev II and clearly shows the wake-affected profiles (sectors 8–12).

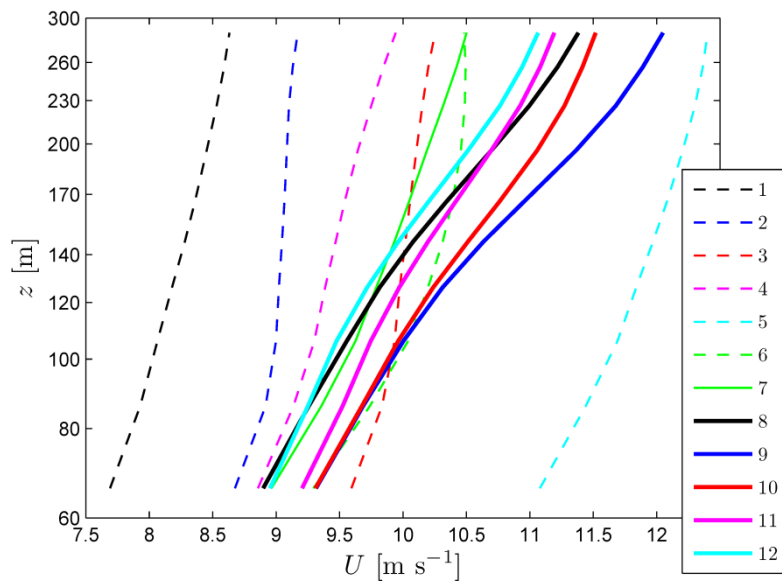


Figure 11: Mean wind speed profiles observed by the wind lidar at Horns Rev II for each of the 12 sectors (from Peña et al., [21])

The analysis was also concentrated in the study of the wind shear exponent at 100 m based on the wind speed profile. Based on all wind lidar observations, distributions of the wind shear exponent ( $\alpha$ ) were inter-compared (see Figure 12). As shown, the shear exponent has a broad distribution, especially the positive side as wind speeds are generally higher with height. Other characteristics found from the investigation were the good amount of negative wind shears and distribution peaks around 0 and 0.05.

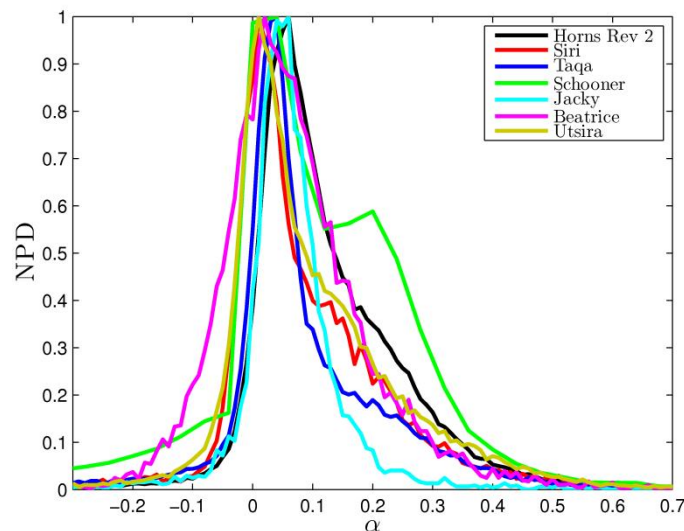


Figure 12: Distributions of wind shear exponents at about 100 m AMSL for a number of wind lidars nodes from the NORSEWInD database (from Hasager et al., [10])

One important result of NORSEWInD was related to the use of mesoscale model outputs together with the observations from the wind lidars. As no measurements of atmospheric stability were available, mesoscale model runs were performed at the wind lidar installations in order to evaluate the state of the atmosphere during the period of the wind lidar deployment. Based on the work of Peña and Hahmann [15], who basically showed that although “instantaneous” measures of stability from numerical mesoscale model output are not accurate enough, long-term stability climatology from such models can be used for vertical extrapolation of the wind, Peña et al. [21] performed the analysis of vertical extrapolation methodologies based on the NORSEWInD wind lidar database. Figure 13 illustrates part of such analysis based on mesoscale model runs and wind lidar observations at Horns Rev II. The “long-term” theory explained by Peña and Hahmann [15] performs very well based on the model outputs (left frame). Thus, when averaging all the wind speed profiles observed at Horns Rev II (right frame), the long-term profile



methodologies performed much better when compared to the observations compared to the traditional neutral wind speed profile.

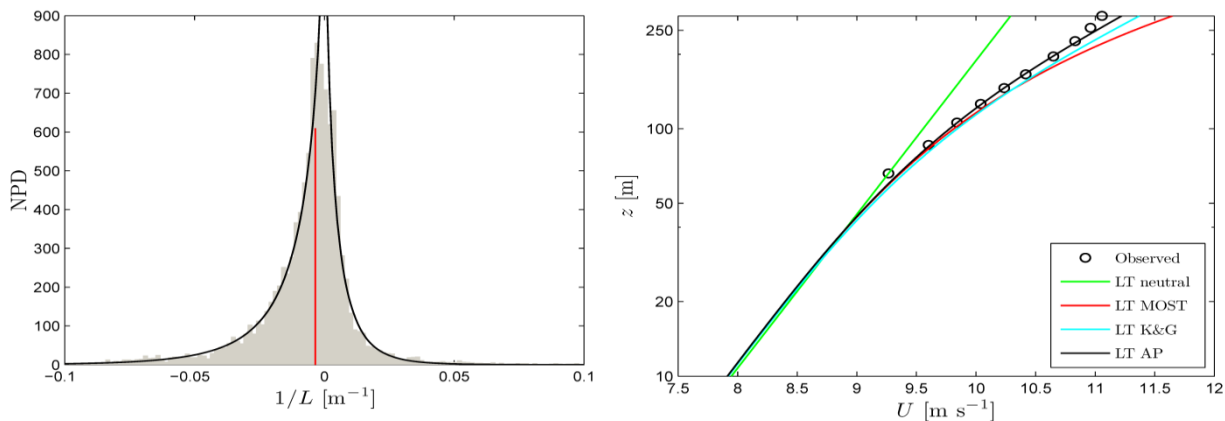


Figure 13: (left) Distribution of the inverse of the Obukhov length ( $1/L$ ) based on mesoscale model outputs at Horns Rev II and (right) long-term vertical wind speed profile observed and modelled at Horns Rev II (from Peña et al., [21])

## 2.6 WINDCUBE AT FINO1 (2009)

### 2.6.1 Objectives, setup and instrumentation

A WindCube wind lidar from Leosphere was positioned on the Fino1 research platform and performed continuous measurements of the wind speed profile from about 100 up to 251 m AMSL from July 2009 to February 2011 (see details in Cañadillas et al. [5] and Muñoz-Esparza et al. [13]). The main objectives of the experimental campaign were to evaluate the performance of the instrument in the offshore environment, to inter-compare the wind lidar measurements with those of the mast (wind speed and turbulence measures), and a more thorough investigation of the vertical structure of the offshore wind profile. Parts of the activities were also related to the evaluation of numerical mesoscale model performance offshore.

### 2.6.2 Results

The overall availability of the wind lidar was about 98% for the overlapping heights (same heights as measured by the cups on the mast) and decreased with increasing height to 91% at 200 m and 83% at 250 m. Correlation analysis shows a good agreement between the wind speeds measured by the wind lidar and the cups and the wind lidar tended to show lower wind speeds. Turbulence comparisons were also performed. Figure 14 illustrates a comparison between the standard deviation of horizontal wind speed measured by the sonic and the wind lidar at 80 m AMSL. The wind lidar measured “more” turbulence at all heights when compared to the sonics. In the figure, turbulence intensity (TI) measured by the sonic and the wind lidar at 80 m is also shown as function of the wind speed measured by the sonic. It is observed that the wind lidar “measured” more turbulence compared to the sonic for the range of wind speeds studied.



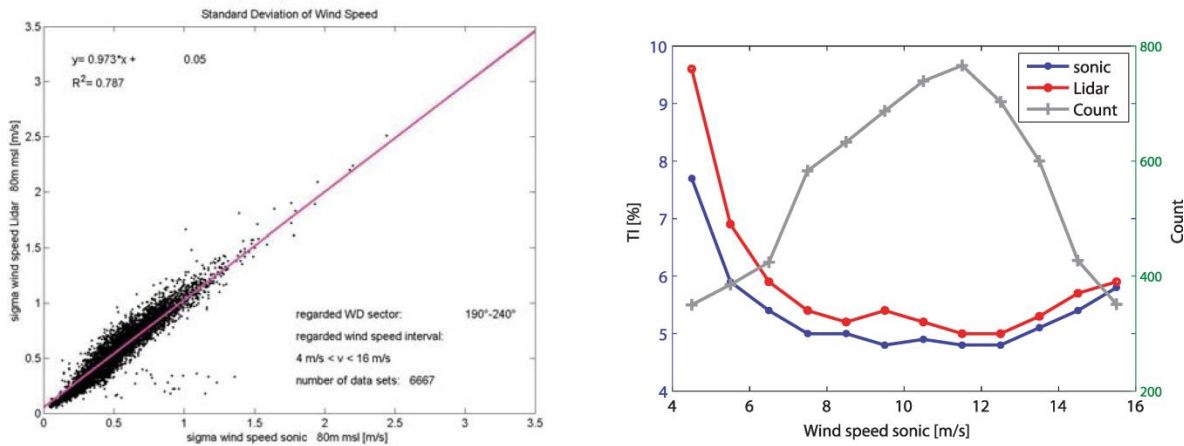


**Figure 14: Comparison of turbulence measures between the wind lidar and a sonic on the Fino1 mast. (Left) Scatter plot of the standard deviation of the horizontal wind speed and (right) turbulence intensities as function of the sonic wind speed (from Cañadillas et al., [5])**

Figure 15 shows the dimensionless profiles observed at Fino1 from combined wind lidar and sonic measurements together with the results of two wind profile parameterizations. It is observed a good agreement between model and observations for the first heights and an increasing bias with height, which is higher for stable conditions (the ones to right side of the graph) compared to unstable conditions.

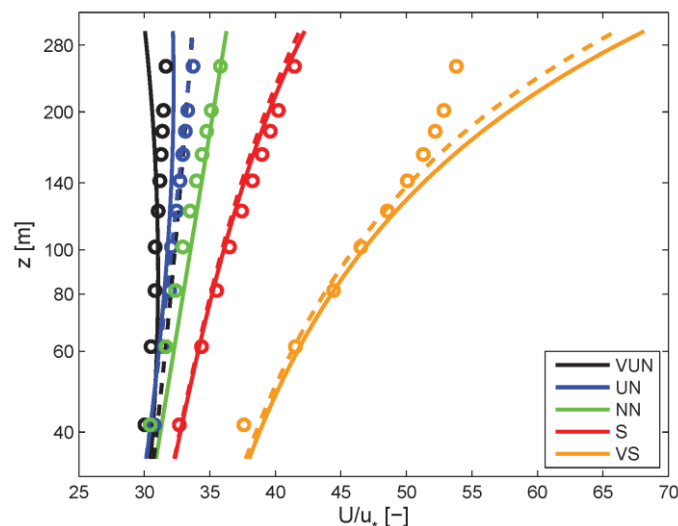


**Figure 15: Non-dimensional wind speed profiles for different stability classes from combined sonic and wind lidar measurements at Fino1. Markers represent the observations and lines the results of two wind profile parameterizations (from Muñoz-Esparza et al., [13])**

## 2.7 ZEPHİR AT FINO3 (2011)

### 2.7.1 Objectives, setup and instrumentation

For the final part of the NORSEWInD project, a ZephIR wind lidar was installed at the Fino3 research platform at the German North Sea. Here we describe the deployment in a separate section as the observations were not part neither of the study of Peña et al. [21] nor of that of Hasager et al. [10], who compiled most of the wind lidar observations of NORSEWInD. It was the first wind lidar deployed at Fino3 and as such the main objectives were, apart from complementing the NORSEWInD dataset, to observe the influence of the mast and the structure on the cup anemometers, to observe the wind profile beyond the top height of the mast (106 m AMSL), and to perform comparisons of the flow distortion and wake generated by the mast with wind tunnel and CFD studies. The wind

lidar observed winds at six heights: 51, 71, 91, 101, 130, and 160 m AMSL from which the first four overlapped cup heights. The period of the campaign at Fino3 was from mid-April to mid-October 2011.

## 2.7.2 Results

For all overlapping heights, it was found a high correlation for the winds speeds observed by the wind lidar and the cups at the mast. However, a 4–5% bias was found at all overlapping heights, i.e. the wind lidar always observed lower wind speeds than the cup (see Figure 16). The reason for that was never found, although it was suspected that the wake of the mast indeed influenced a part of the wind lidar observations, as these are taken conically around the mast.

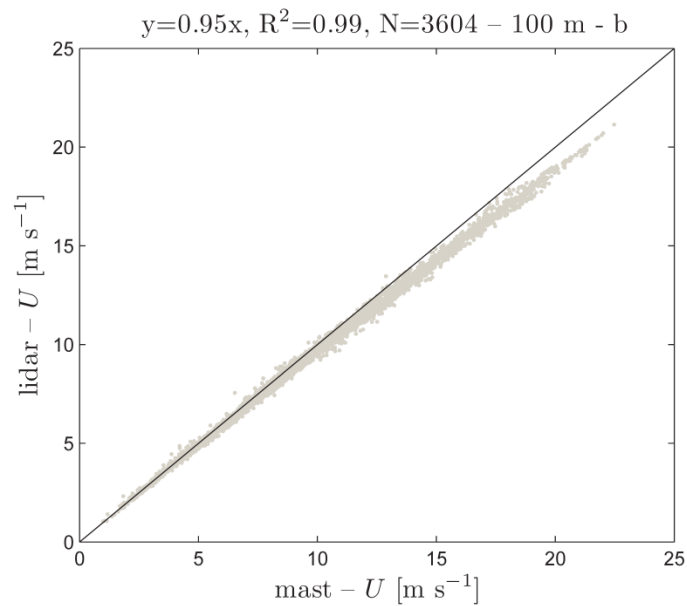


**Figure 16: Comparison of 10-min horizontal wind speeds measured by the ZephIR wind lidar and the cup anemometer at 100 m AMSL at Fino3**

Unfortunately, the raw fast data of these wind lidar were not accessible and so it became difficult to find out whether it was the mast itself, which influenced the wind lidar measurements. A snap shot of the so-called figure of height for the lowest height (25 m over the system; 51 m AMSL) actually shows the wake of the mast on the wind lidar radial velocity scans (see Figure 17).

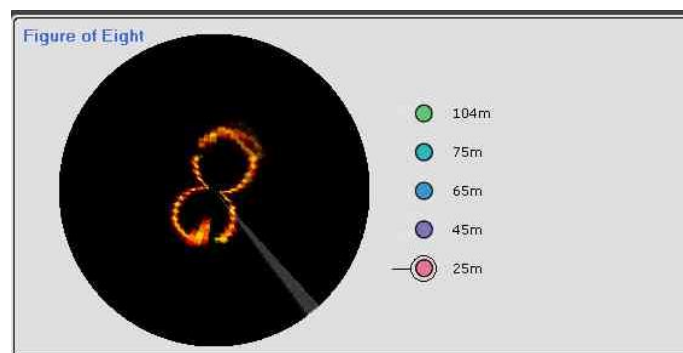


**Figure 17: Figure of eight of radial velocities of the ZephIR wind lidar at Fino3 for the lowest measurement height (courtesy of Detlev Stein-GL Garrad Hassan)**

## 2.8 TALL WIND PROFILE OFFSHORE EXPERIMENT (2013)

### 2.8.1 Objectives, setup and instrumentation

As part of the tall wind profile project, a measurement campaign was very recently initiated at the Fino3 research platform at the German North Sea. The project's aim is to observe the behaviour of the wind speed profile and the turning of the wind in the entire ABL. Therefore, the measurements are performed with a "long-range" pulsed wind lidar (WLS70 from Leosphere), which is able to measure wind speed, direction, and turbulence from 100 up to 2000 m, depending on the aerosol content in the atmosphere. The objective is to complement the wind lidar measurements with those of the meteorological mast at Fino3 (from 30 up to 106 m AMSL) to study for the first time the behaviour of the wind speed profile in the whole marine ABL. Also, measurements from a ceilometer (Vaisala CL51) are concurrently carried out at Fino3. Such observations have been used previously to estimate the BLH (see Peña et al., [18]). Details related to the wind lidar and results from onshore experiments developed during the Tall Wind project are given in Floors et al. [8] and Peña et al. [17]. The campaign started at the end of August 2013 and will run for six months.

### 2.8.2 Results

First results of the offshore campaign are shown in Figure 18 and Figure 19. In the first the aerosol backscatter (colormap) observed by the CL 31 ceilometer during one day (3<sup>rd</sup> of September 2013) is given for the heights in which the BLH is probably located. The colormap is truncated to 250 to be able to observe the layers with lower aerosol content (cloud formations are normally found above these threshold).

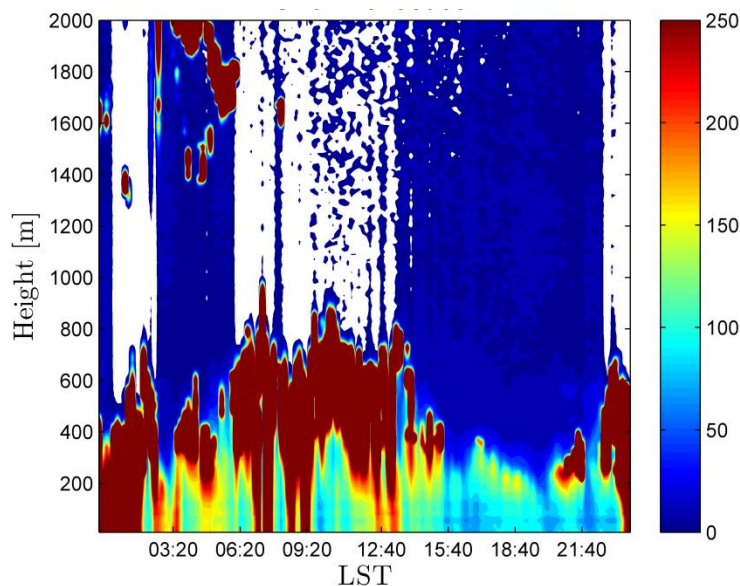


**Figure 18: Observations of the aerosol backscatter from a CL51 ceilometer for September 3, 2013, at the Fino3 platform**

Figure 19 illustrates some of the first vertical profiles of the relative wind direction change and the magnitude of the horizontal wind speed of the wind lidar at Fino3. As observed wind direction changes up to 40° in magnitude from 100 to 1000 m and the wind speed shows a close to logarithmic shape with very high magnitudes (the mean wind speed at 100 m is above 10 m s<sup>-1</sup>).

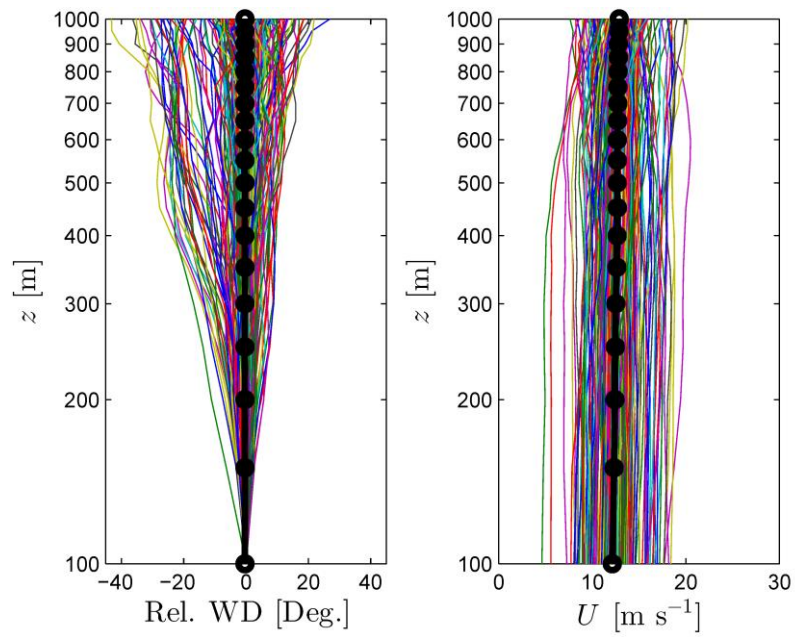


Figure 19: Vertical profiles of the relative wind direction change (left) and the horizontal wind speed magnitude (right) at Fino3

## 3 SCANNING LIDAR MEASUREMENTS FROM COASTAL SITES

### 3.1 INTRODUCTION

Large amounts of wind energy are being installed offshore. Due to lower water depths, lower transmission cable lengths and cheaper operation and maintenance, it is economically attractive to build wind farms close to the coast. In these areas, within 10km of the coastline, one possibility for measuring the available resource is to use sector-scanning lidars or dual-doppler scanning lidars (see [6], section 2.7). The lidars would be positioned on-shore at coastal vantage points but would be able to measure the wind speed up to 10km offshore. Both techniques are rather new since the necessary lidars are only recently available on the market. The advantages over traditional mast based offshore instrumentation are likely to be significantly lower costs and a much quicker deployment time.

Here we report on an experiment designed to test the feasibility of sector-scanning lidar measurements. The measurement principle is shown in Figure 20. One lidar scans over a sector of 30- 50° width at the desired range (or ranges). The assumption is that (at a given range) the wind speed and direction remain the same, in which case the different LOS directions will see different projections of the same wind speed (as shown in the inset in Figure 20). In order to give the horizontal wind speed and wind direction, the radial wind speeds from each LOS direction would be fitted to a cosine curve, the amplitude giving the wind speed and the phase giving the wind direction. Typical reconstruction algorithms are found in [7].

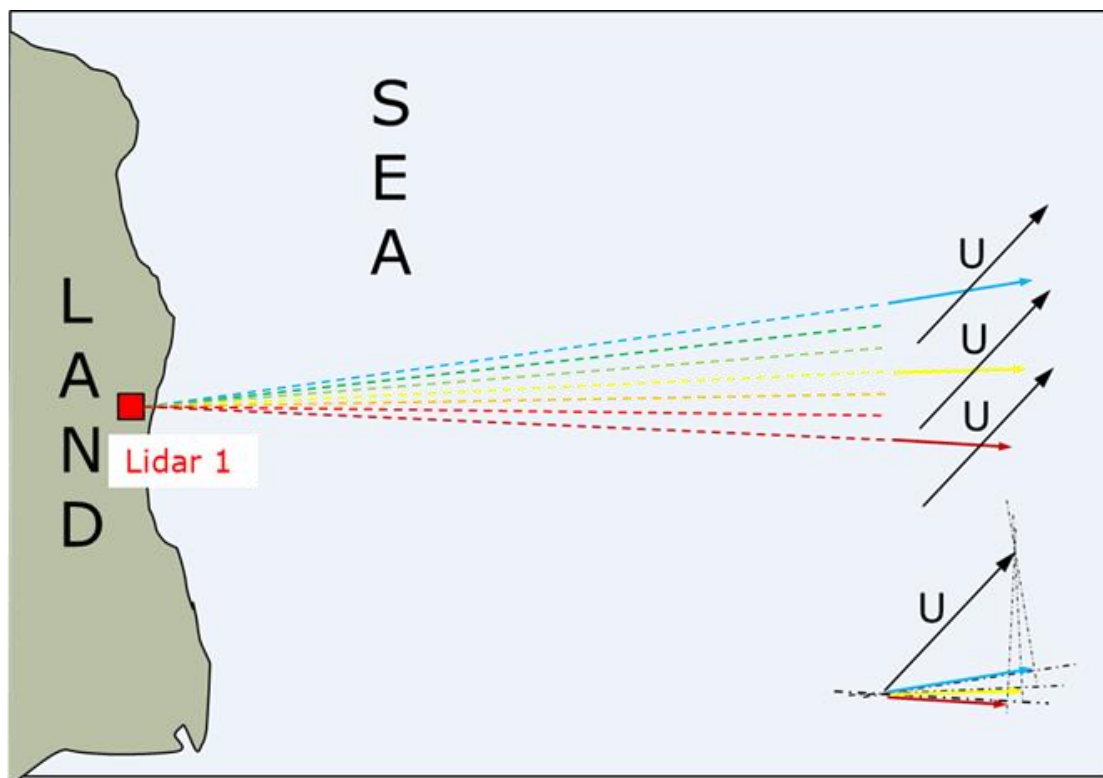
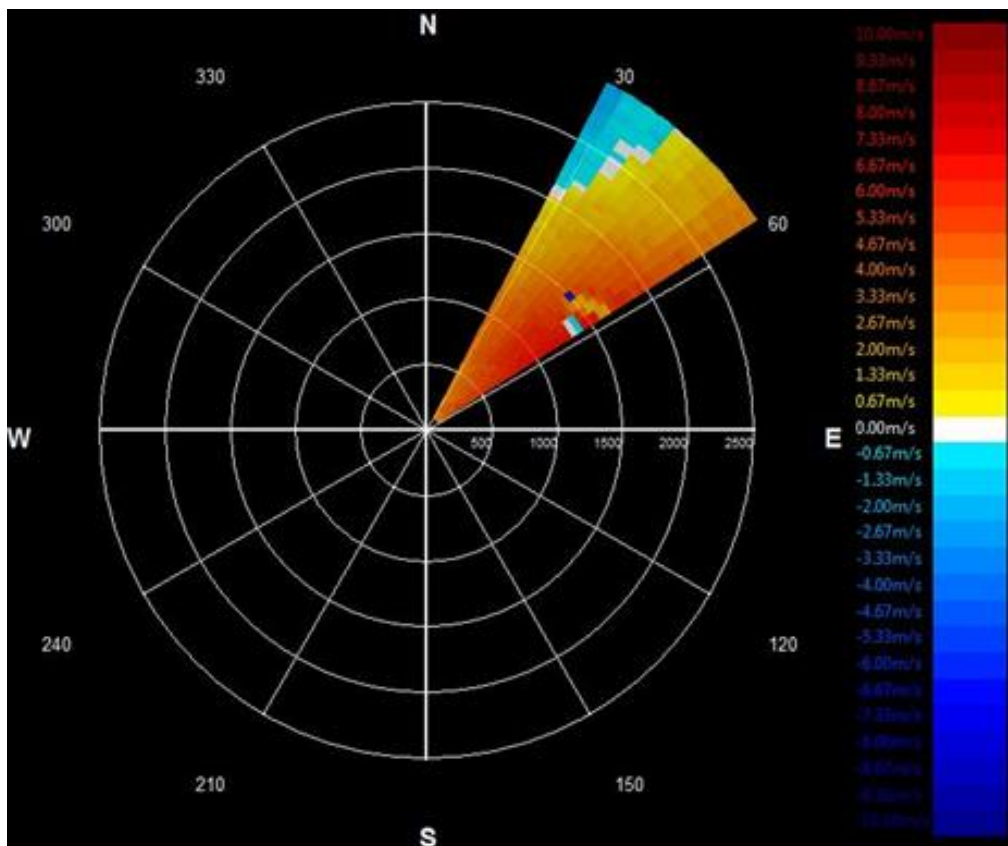


Figure 20 Sector-scanning lidar measurements of near-coast wind speed.

In this project, this approach has been tested onshore by comparing the wind speed and direction measurement by a scanning lidar to a cup anemometer and a vane mounted on a met tower. A Windcube 200S was installed at 1.6km from a high quality met tower. As long as the flow conditions around the met tower (within the sector scanned by the lidar beam) are sensibly homogeneous, onshore testing should give meaningful results. Offshore, the local homogeneity condition will be easily fulfilled as long as there are no local wind farms or unless the orography of the coastline is strongly three-dimensional.

The scanning pattern used in sector-scanning is known as Plan Position Indicator (PPI). The beam elevation angle is held constant (this determines the sensing height at a given range) and the beam is scanned in an azimuth sector. One of the aims of this experiment is to investigate what influence the sector size has on the quality of the derived wind speeds. Both 30° (Figure 21) and 45° (Figure 22) sectors have been investigated. For larger sector sizes, the homogeneity assumption becomes increasingly violated and for smaller sector sizes we anticipate that the small differences in radial speed will give too uncertain horizontal wind speed estimates.

For a given sector size, another relevant parameter is how quickly the sector is scanned. Since the lidar can acquire data at a given maximum rate (here 1Hz) the angular speed of the beam determines how many different radial speeds are measured inside a given sector. A low angular speed will result in a larger number of individual angles inside the sector. On the other hand a fast speed will give fewer discrete angles but higher statistical certainty for each angle since the sector can be scanned more times in the given 10 minute period. Scanning speed will be varied in this experiment in order to examine the effect of this parameter.



**Figure 21** Example of PPI scan with an azimuth range of 30°, centered on 42.5° (elevation: 4.2°). The radial axis is range in meters.



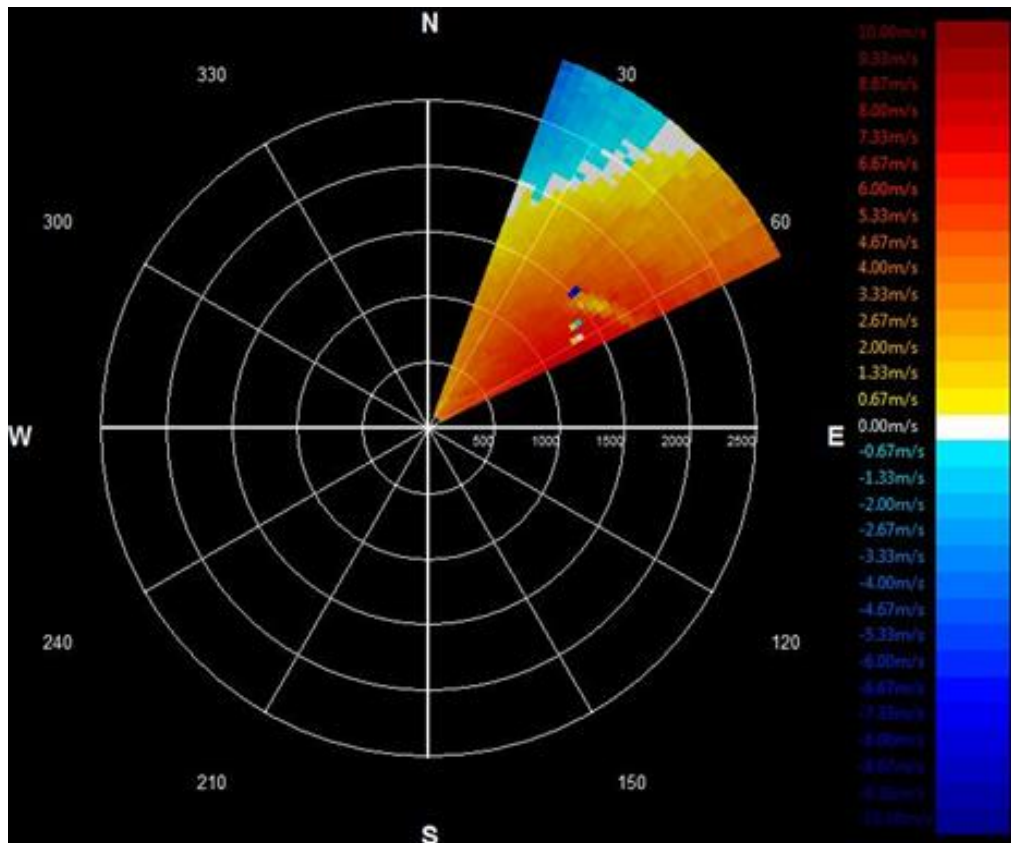


Figure 22 Example of PPI scan with an azimuth range of 45°, centered on 42.5° (elevation: 4.2°). The radial axis is range in meters.

In the remainder of this report we describe the test site and reference instrumentation in section 3.2, the test setup in section 3.3, the results from the scanning experiments in section 3.4 and some conclusions in section 3.5.

### 3.2 TEST SITE AND INSTRUMENTATION

The test was performed at the Danish National Test Station for Large Wind Turbines, located at Høvsøre in Western Jutland, Denmark, about 30 km west-northwest of Holstebro.

The facility comprises a line of five test stands for MW-class wind turbines, oriented north-south parallel to the coast (slightly, about 3 deg, tilted to the east), and each stand has its dedicated upstream measuring mast for power performance tests to the west. The lidar tests used a 116.5m met mast at the southern end of the turbine row and 200 m from the closest wind turbine – see Figure 23 and Figure 24.

Høvsøre is a flat site, mainly consisting of grasslands, with maximum height variations less than 5 m. To the south is a lagoon, at the closest point 900 m from the met. mast. The site is about 1.8 km to the west of the North Sea, separated from the land by a strip of sand dunes about 10 m high – see Figure 25. The land behind the dike lies about 1-5 m above sea level.

Wind speed is taken from an instrument mounted on the top of the mast at 116.5m. This is a Windsensor P2546a cup anemometer with a calibration from Deutsche Windguard. The wind direction reference is from a vane at 100m on a south facing boom.

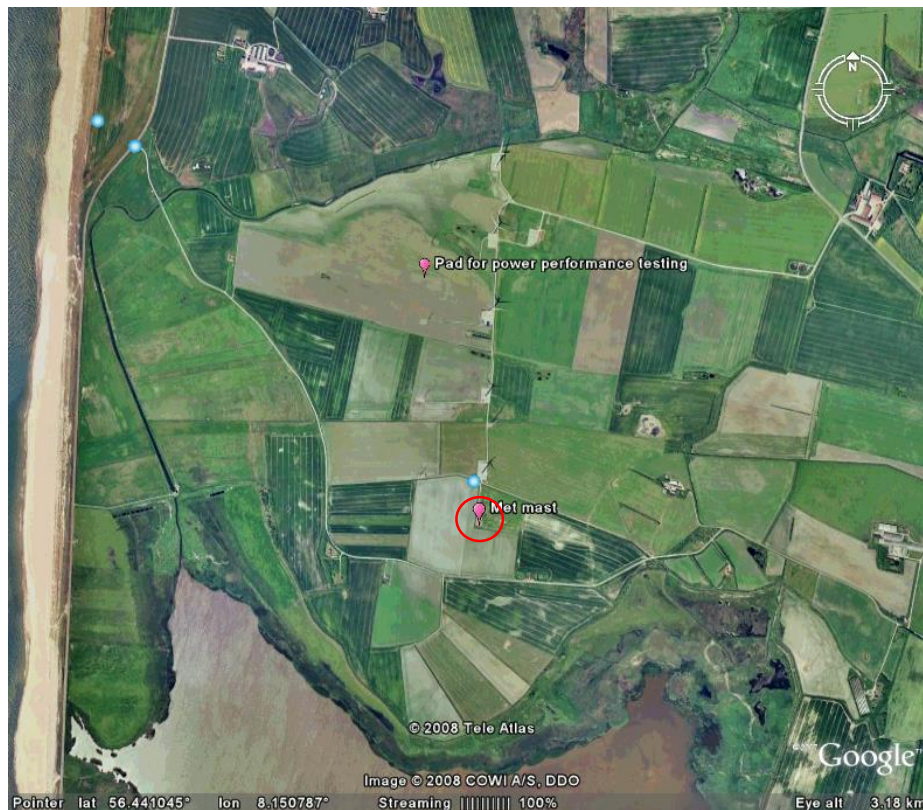


Figure 23 Outline of Høvsøre test site (picture from Google Earth). The met. mast used for the reference measurements is marked by the red circle.



Figure 24 The row of wind turbines at the Høvsøre test site with the tall met. mast in the front.





Figure 25 Høvsøre test site seen from the coastline to the west.

### 3.3 THE TEST SETUP

The aim of the measurement campaign was to compare the wind speed and direction measured by the scanning lidar to those measured at the top of the met mast. A distance of 1.6km was selected as this represent a rather short but not unrealistic near-shore scanning distance and allows the equipment to remain within the confines of the Høvsøre test station. The scanning lidar, a Leosphere Windcube 200S (Figure 27) was placed on the north side of the entrance road to the test site and aimed towards the met mast at the southern end of the turbine row (see Figure 26). There is an un-disturbed view in this direction (Figure 28) and the distance between the lidar and the met mast is 1615.6 m. The relevant coordinates are given in Table 1.

The lidar software and reference instruments data acquisition were synchronized to the same time server at least once every hour. Possible time deviations between the two systems were less than 10 s.



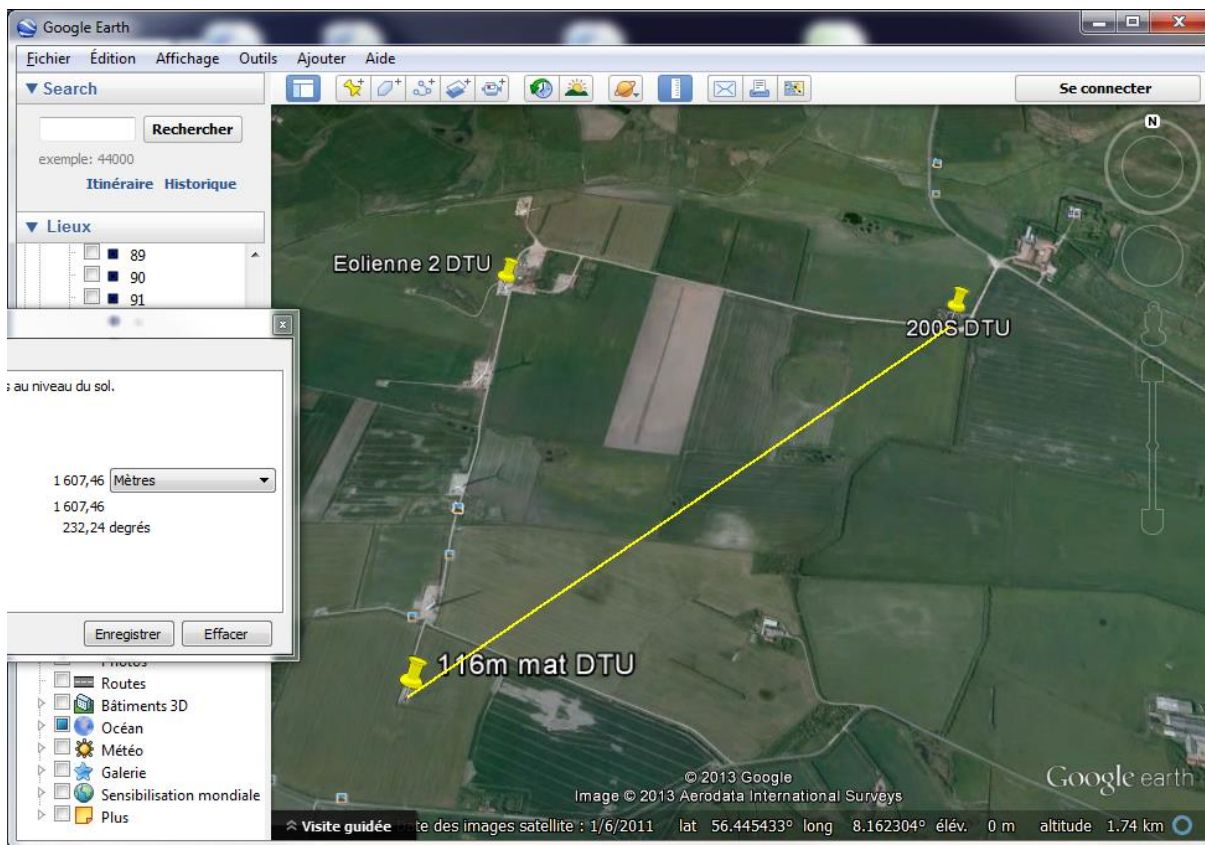


Figure 26 Google picture of Høvsøre test station for large wind turbines, with location of the lidar and the met mast



Figure 27 The lidar installation by the side of the road.



**Figure 28** The view from the lidar site towards the met mast (indicated with a circle).

### 3.3.1 Leveling the lidar

In coastal scanning lidar measurements, the accuracy of the elevation angle largely determines the obtainable measurement uncertainty. Any elevation angle error will translate to a sensing height error and depending on the severity of the shear; a wind speed error will result. Much attention has been paid to the initial leveling.

The lidar pitch and roll have been adjusted with an electronic spirit level, having an accuracy of  $0.05^\circ$ . The level was placed on the plate attached to the optic unit of the lidar including the laser and the scanning head. It has shown a horizontality of  $0.00^\circ$  to  $0.05^\circ$  (see Figure 29). The variation of the pitch and roll angles have also been measured while the scanning head was rotating; to verify their sensitivity during the measurements. Good stability was found, with the leveling remaining within the  $0.00^\circ$  to  $0.05^\circ$  initially indicated by the spirit level.

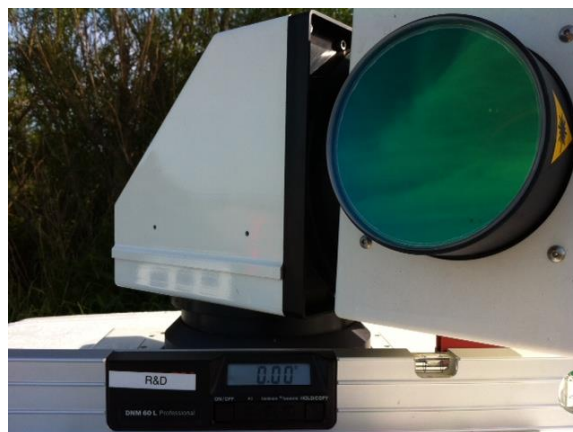


**Figure 29** Picture of the electronic spirit level while checking the WLS2005 levelling.



### 3.3.2 Verification of the lidar azimuth angle indication

A PPI scan was performed for a vertical angle of  $1^\circ$  above the horizontal and an azimuth angle between  $65^\circ$  and  $80^\circ$ . According to the resulting CNR and radial wind speed maps, wind turbine 3 appeared (as a low CNR dot, resp. a low radial speed dot right behind the obstacle) at about  $73^\circ$  azimuth relative to the lidar (Figure 30). Since it is not possible to read the azimuth of the turbine position accurately in the PPI scan figure, a sequence of LOS scans with a fixed elevation angle of  $1^\circ$  and azimuth angle varying from  $72.5^\circ$  to  $73.5^\circ$  was used to find the position of the turbine more accurately. When the lidar beam hits the wind turbine, it appears as a high peak in the CNR profile, at a range of about 1400m. The position of the turbine relative to the lidar was found to be at  $72.9^\circ$ - $73.0^\circ$ .

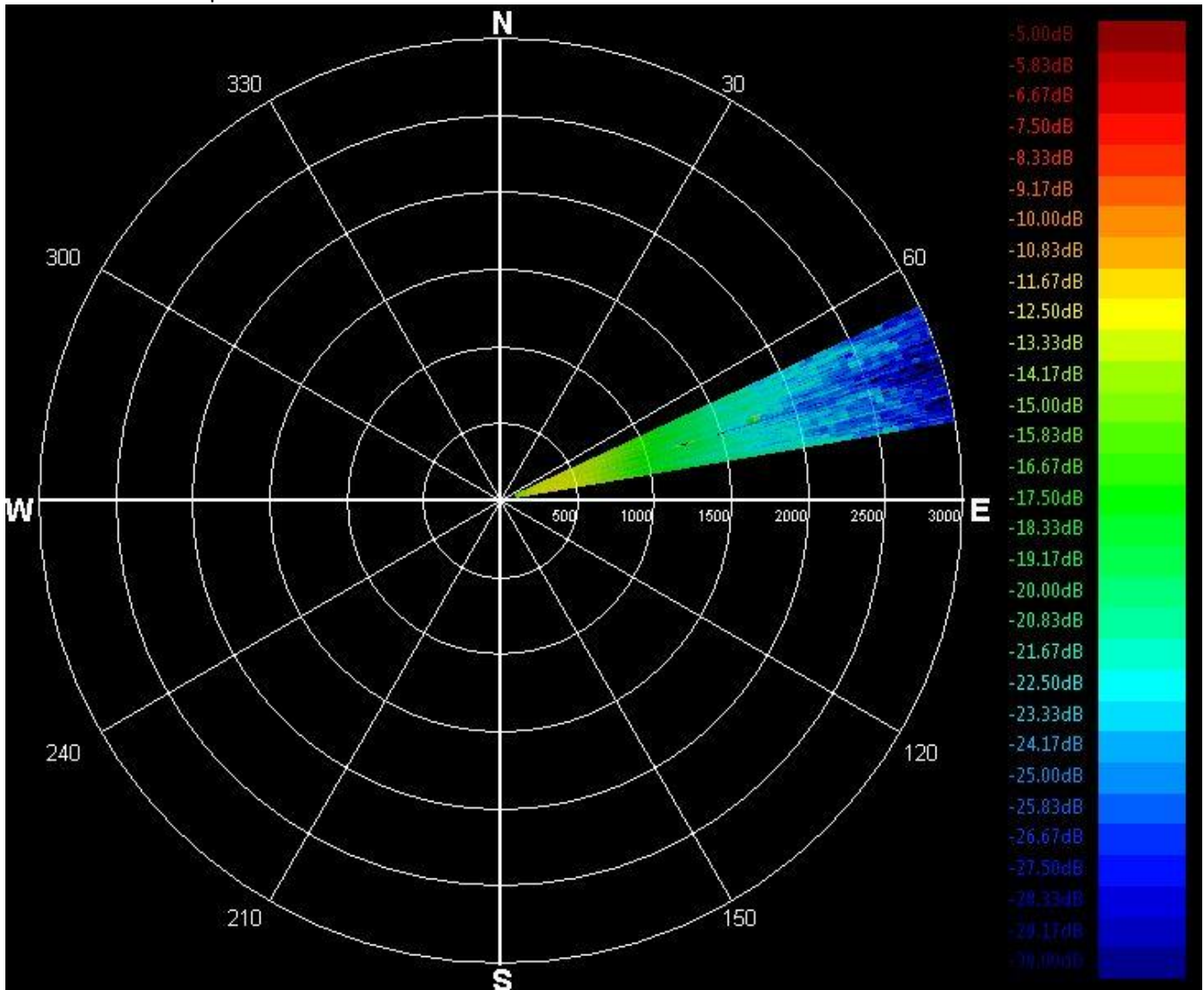


**Figure 30** CNR map of a PPI scan for a vertical angle of  $1^\circ$  above the horizontal and an azimuth angle between  $65^\circ$  and  $80^\circ$ . Wind turbine 3 appears as a black dot (very low CNR right behind the obstacle) at about  $73^\circ$  azimuth and 1350m range.

On the other hand, the actual direction between the lidar position and wind turbine 3 was calculated from their coordinates:  $262.9^\circ$ . The lidar direction offset (lidar  $0^\circ$  azimuth angle toward geographic north) was therefore deduced to be  $189.9^\circ$ .

The direction offset has then been verified by comparing the actual position and that found with the lidar CNR for Wind Turbine n.4 and the north light mast. The detected positions of these hard targets have shown an azimuth positioning accuracy of the order  $0.1^\circ$ , which is the smallest possible increment in the internal lidar software.

### 3.3.3 Verification of the lidar scanner head elevation angle

The north light mast is 165m high and is located at 1211m from the lidar at a relative azimuth position of 92.07°. The elevation angle to reach the top of the mast from the lidar position is therefore 7.76°. Whilst the width of the mast base is about 4m, the mast decreases in width with height and is only about 1m in width at the top. With an azimuth resolution of 0.1°, a width of  $1211 \cdot \tan(0.1^\circ) = 2.1\text{m}$  is required to give robust detection of the mast. It is therefore very difficult accurately to detect the top of the mast with a RHI scan. Therefore, we performed a series of PPI scans, with an azimuth angle range from 91.9° to 92.1°, with an increment of 0.1°, for the elevation angles 7.7°, 7.8° and 7.9°. The mast could still be seen for an elevation angle of 7.8° but not 7.9°. The elevation angle is therefore given with an accuracy of 0.1° to 0.15°.

The effect of the scanner head gearbox backlash could clearly be seen. When scanning with increasing elevation angle sequence, the mast top could be detected at an elevation angle of 7.8° but not with a decreasing elevation angle sequence when it could first be detected at 7.7°.

### 3.3.4 Met mast azimuth and elevation angles

With the same processes as described in 3.3.2 and 3.3.3, the azimuth position of the met mast relative to the lidar position was found to be 42.5°. The calculated elevation angle for the beam to hit the top of the mast is 4.12° considering no topographic elevation differences between the lidar and the mast. The lidar beam hit the mast for an elevation angle smaller and equal to 4.1° but not for 4.2°, confirming correct leveling of the lidar and no significant elevation change between the mast and the lidar position.

## 3.4 RESULTS

### 3.4.1 Verification of the consistency of the beam orientation

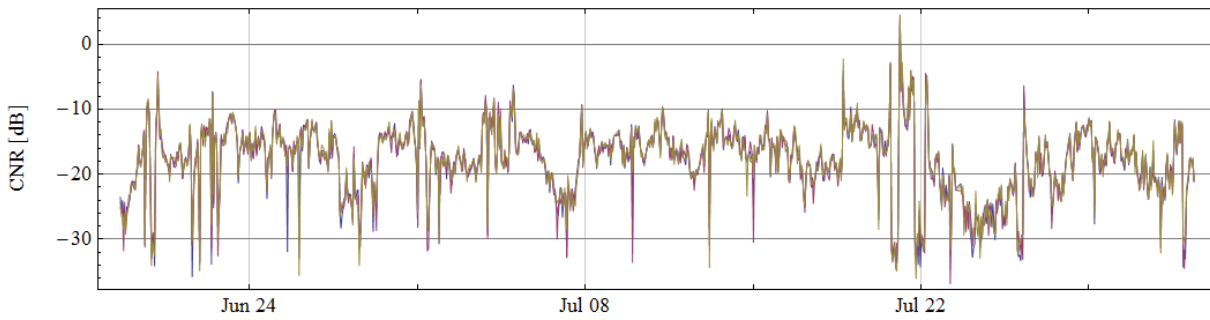
Throughout the campaign, measurements were made to check that the azimuth and elevation angles remained consistent. Settling of the lidar or other inaccuracies could otherwise subtly alter the lidar beam positioning accuracy. Here we first show measurements demonstrating that the azimuthal orientation of the lidar did not change during the period. Subsequently we demonstrate also that the elevation angle has remained consistent for the duration of the campaign.

Figure 31 shows time series of the CNR for a LOS elevation angle of 3.5° for three different azimuth angles 42.25, 42.5 and 42.75 (red, blue and yellow respectively) for a total of four different range setting (1550m, 1600m, 1650m and 1700m), one in each pane. At 1550m range, the lidar beam does not intercept the mast and the CNR is sensibly identical for all the azimuth positions (the colours merge to brown). At 1600m range, the CNR for the 42.5° azimuth position (blue) is much higher than for the other azimuth positions, showing that the laser beam clearly hits the met mast when the beam is pointing in this direction. At 1650m range, the CNR for the 42.5° azimuth position is still clearly higher than for the other azimuth positions but not as high as for the 1650m range. At 1700m range, the CNR is again sensibly identical for all azimuth positions since at this distance, the range gate is behind the met mast.

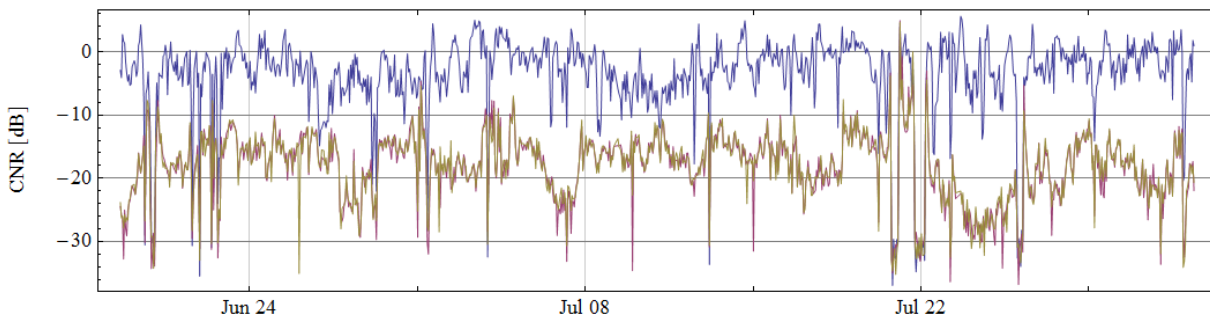
Figure 32 also shows a time series of the CNR, but here the CNR level is indicated by a colour (red is high, blue is low) and the y-axis is used to show the CNR variation with azimuth angle. Again different ranges (1550m, 1600m, 1650m and 1700m) are shown in separate panes. Figure 32 shows that:

- The CNR is sensibly the same for all azimuth position swept in this PPI scan; the aerosol distribution is spatially homogeneous;
- However, the CNR can vary widely from time to time
- The laser clearly hits the mast for an azimuth position of 42.5 at the 1600m range, which confirms the azimuth orientation of the lidar scanning head.

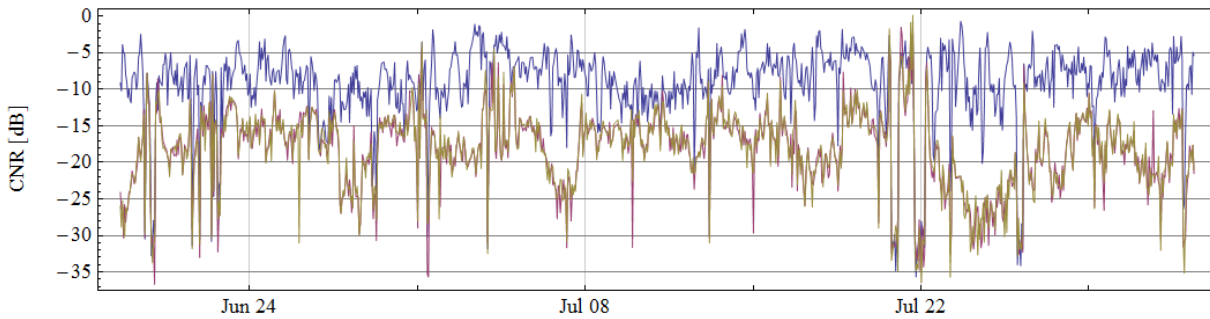
Elevation: 3.5° – Range: 1550 m



Elevation: 3.5° – Range: 1600 m



Elevation: 3.5° – Range: 1650 m



Elevation: 3.5° – Range: 1700 m

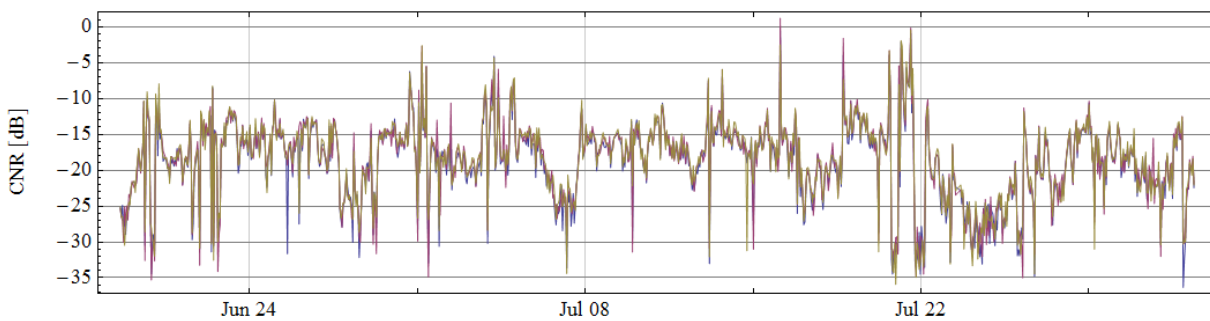


Figure 31 Time series of the CNR for LOS elevation angle of 3.5°, 3 different azimuth angles: 42.25 (red), 42.5 (blue), 42.75 (yellow) and 4 different ranges (from top to bottom): 1550, 1600, 1650 and 1750.



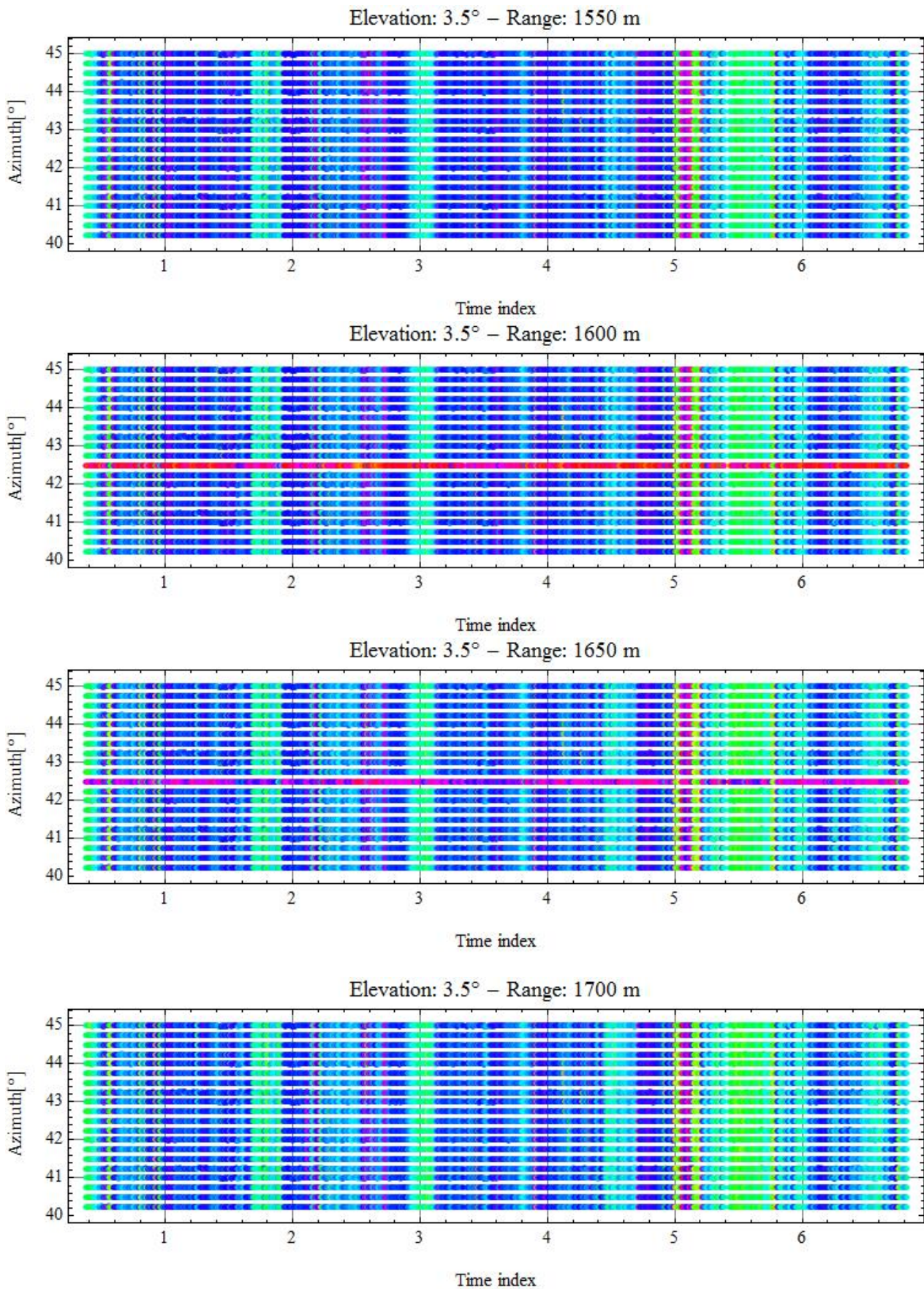
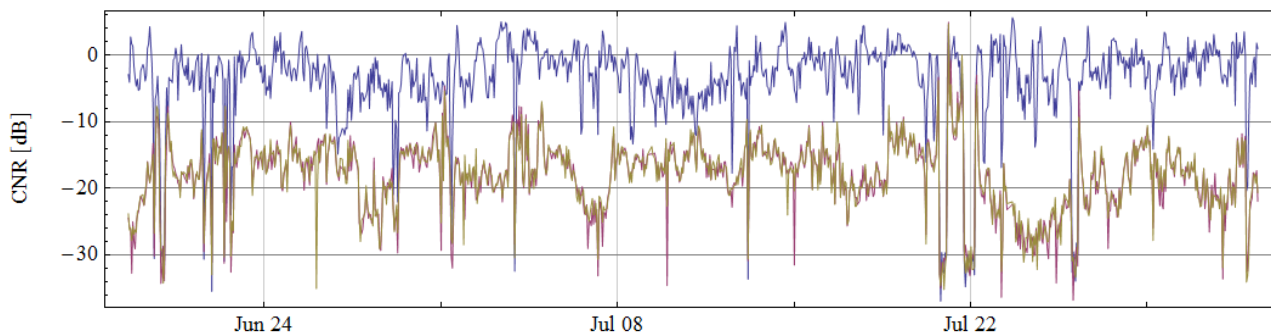


Figure 32 Time series of the CNR (displayed as color from dark blue for low CNR to red for very high CNR) for the LOS elevation angle of 3.5° and all azimuth angles between 40.25 and 45. The four plots show the measurements taken at 4 different ranges (from top to bottom): 1550, 1600, 1650 and 1750m.

Elevation: 4.0° – Range: 1600 m



**Figure 33** Time series of the CNR for LOS elevation angle of 4.0°, 3 different azimuth angles: 42.25 (red), 42.5 (blue), 42.75 (yellow) and at the measurement range 1600m.

Figure 33 shows a plot of CNR as a time series similar to the sequences in Figure 31 but here at an elevation angle of 4° (previously at 3.5°) and only for the 1600m range (the range closest to the mast). Like at 3.5° elevation angle, the lidar beam clearly hits the mast for the azimuth angle 42.5°, except a couple of times where the CNR drops to the same CNR as the surrounding azimuth positions as if it missed the met mast. At 4° elevation, the beam intersects the mast at about 112m where it is significantly narrower than at the intersection height for 3.5° (99m).

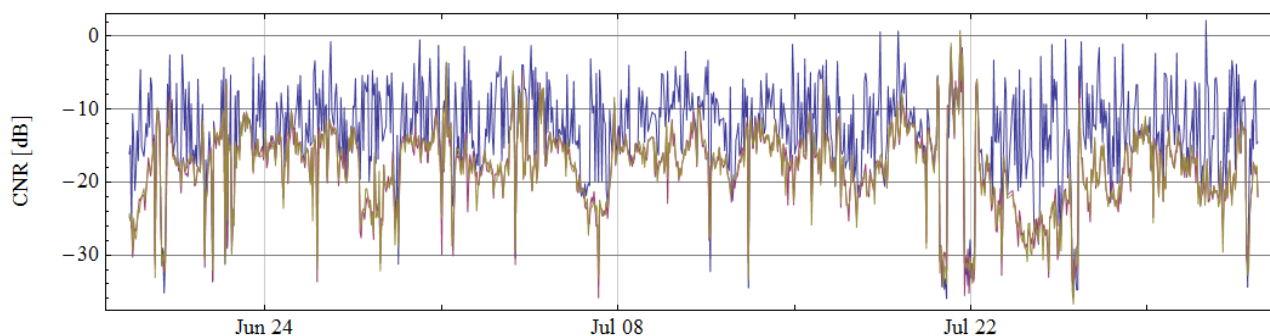


**Figure 34** Time series of the CNR for LOS elevation angle of 4.1°, 3 different azimuth angles: 42.25 (red), 42.5 (blue), 42.75 (yellow) and the measurement range 1600m.

In Figure 34, the elevation angle has increased from 4.0° (Figure 33) to 4.1°. Now the laser beam seems to partially hit the met mast or maybe the top cup anemometer, since the CNR for the azimuth position 42.5° is higher than for the other azimuth angles, but only by a few dB.



Elevation: 4.2° – Range: 1600 m

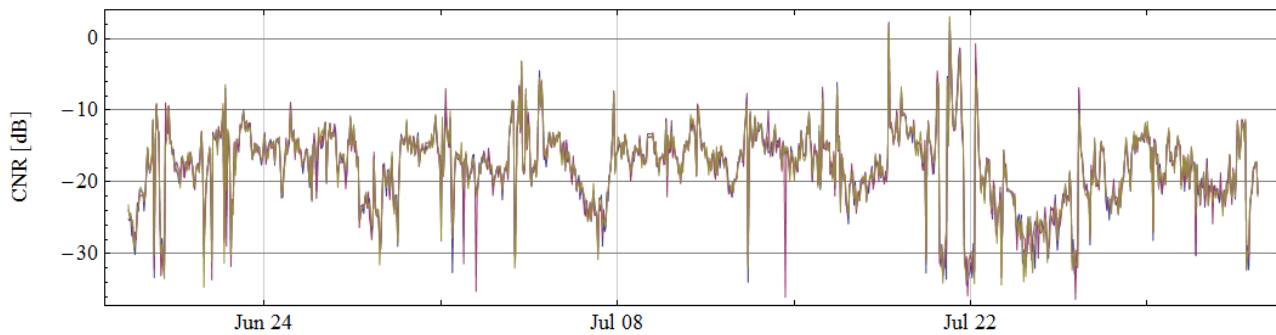


**Figure 35** Time series of the CNR for LOS elevation angle of 4.2°, 3 different azimuth angles: 42.25 (red), 42.5(blue), 42.75 (yellow) and the measurement range 1600m.

In Figure 35 the elevation angle has increased once more to 4.2°. At this elevation angle, the laser beam crosses the mast position at 118m above the surface and therefore does not hit the mast at all (the top cup anemometer is at 116.5m). This is demonstrated by the sensibly identical CNR for all azimuth positions.

Figure 33, Figure 34 and Figure 35 confirm that the elevation accuracy of the scanning head remains unchanged for the duration of the campaign. There is no evidence of any settling of the lidar that could otherwise have altered the beam inclination.

### 3.4.2 Radial wind speed measurement

Having ascertained correct and consistent alignment of the scanning geometry, the next step is to show that the radial speed measured by the lidar is consistent with the known geometry and the horizontal wind speed and direction measured by the reference instruments on the met mast. In order to achieve this, a number of ‘staring’ trajectories were regularly performed in which, for ten minutes, the lidar beam would be pointed directly towards the mast with no imposed scanning. The wind speed and direction distributions of the raw dataset available for this line-of-sight (LOS) comparison are shown in Figure 36 and Figure 37 respectively. Figure 38 shows a scatter plot of wind speed vs direction for this dataset.

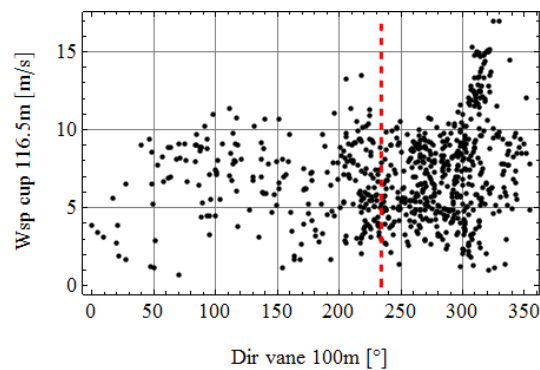
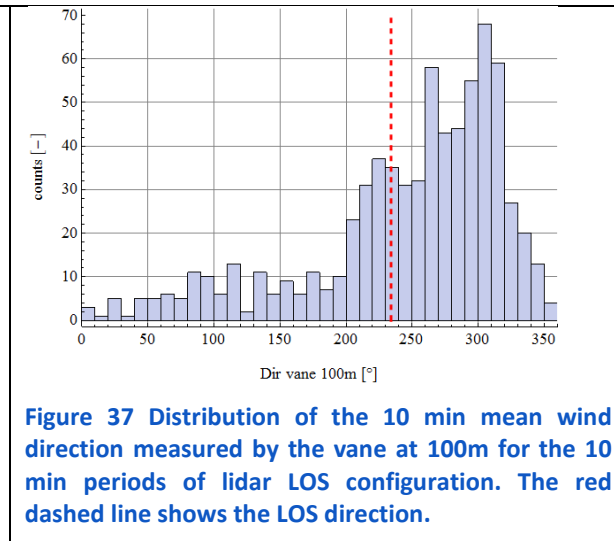
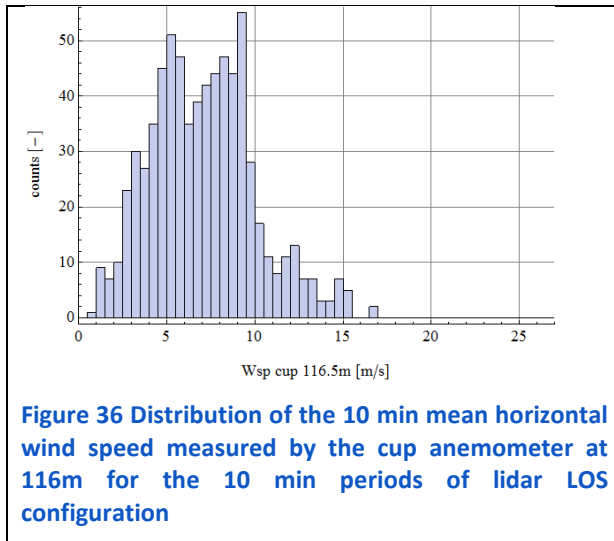


**Figure 38** 10 min mean horizontal wind speed measured by the cup anemometer at 116m vs wind direction measured by the vane at 100m for the 10 min periods of lidar LOS configuration. The red dashed line shows the LOS direction.

In order to demonstrate that the lidar is also measuring at the correct range, a cross-correlation has been performed between the 10 minute averaged radial wind speeds and the projection of the 10 minute averaged cup wind speed (116m) in the LOS direction. The mean wind speed at 100m is used in the calculation of the projected wind speed. Results for the cross-correlation are shown in Figure 39. It can be seen that the highest correlation occurs at the lidar range corresponding to the distance between the lidar and the mast. This confirms the range accuracy of the lidar.

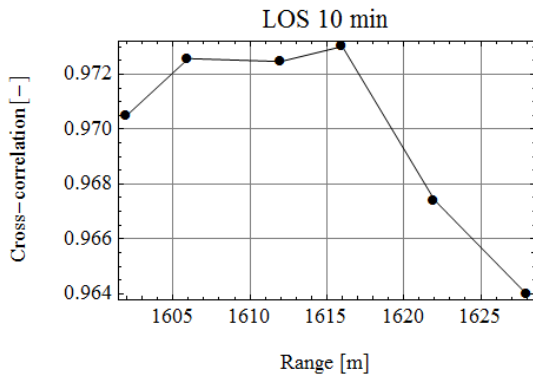
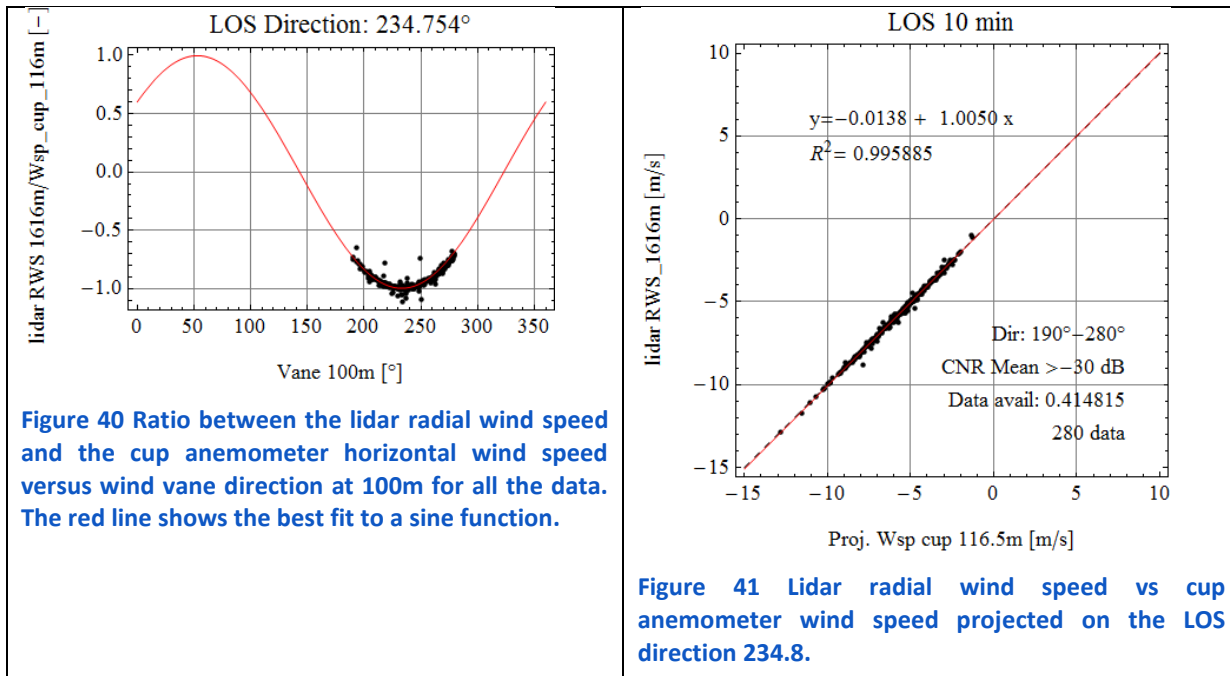


**Figure 39** Cross-correlation between the 10 min lidar radial wind speed and the 10 min mean wind speed measured by the cup anemometer at 116m projected on the lidar LOS direction, for 6 different measurement ranges.

Before performing the regression analysis between the lidar radial speeds and projected cup speeds, a number of steps were performed. Firstly the data were filtered to remove invalid radial speeds (0.0 values) and also filtered so as to retain only wind from the sector 190-280°. This direction filtering removes all significant wind turbine wakes and also maximizes the correlation between the radial and projected speeds. Lastly periods with a lidar signal to noise ratio (CNR) of less than 30dB were also omitted as these were seen to be clearly correlated with increased scatter.

A cosine function was fitted to the filtered data, and the exact line-of-site determined from this to be 234.8° (Figure 40). Using this angle for the projection, a linear regression was performed between the lidar radial speeds and the projected cup anemometer speeds (Figure 41). There is excellent agreement with an offset of -0.01m/s and a gain error of 0.5%. Thus the veracity of both the scanning geometry and the radial wind speed measurement has been demonstrated.



### 3.4.3 Sector scanning results

Having ascertained the correct scanning geometry and checked the accuracy of the line-of-sight wind speeds it is now meaningful to examine how well the lidar can measure when performing sector-scanning. In order to study the influence of both the size of the scanning sector and the speed at which the sector is scanned, four different PPI trajectories have been implemented (scan 1 to scan 4). These are defined in Table 1. Note that in all four cases, the elevation angle is constant at 4.2° so that (with the 1616m range) the centre of the probed volume is just above the top of the met mast.

**Table 1 Properties of the 4 PPI scanning trajectories.**

Scan number	Swept angle [°]	Scanning speed [°/s]	Scans/ 10mins	Elevation angle [°]
Scan 1	30	2	40	4.2
Scan 2	30	3	60	4.2
Scan 3	45	2	26	4.2
Scan 4	45	3	40	4.2

A sequential program of different scanning scenarios was employed, interspersed with periods of staring (LOS) and position check trajectories. Each of the PPI scanning scenarios was ten minutes in length and each of these datasets have been processed to one ten minute value of mean wind speed and direction. The speed reconstruction is basically a fitting of the radial speeds in the different directions to a cosine in order to obtain speed (amplitude) and wind direction (phase). However the precise details remain a proprietary secret of Leosphere.

#### 3.4.3.1 Horizontal wind speed and wind direction

Radial wind speeds were processed off-line by the lidar manufacturer using a proprietary algorithm. The results shown here are from a second version of the processing software where the algorithm has already been de-bugged and improved by comparison with the mast data from this campaign. We believe that this dataset is fairly representative of the measuring performance available with sector scanning lidars.

A linear regression was performed between the 10 minute mean horizontal wind speed lidar measurements and the cup anemometer 10 min mean wind speed for each scan (1 to 4). The 10 minute time periods were selected based on the lidar PPI scanning time period for both the lidar and the cup anemometer.

In the results shown, Figure 42, only data from a limited number of sectors has been shown. The wind sector was selected so that the reference cup anemometer was not in the wake of the wind turbines (60-300) and the wind direction was not orthogonal to the lidar beam ( $234.5+22.5-90=167^\circ$  to  $234.5-22.5+90=302^\circ$ ). The final wind sector used for the lidar-cup anemometer comparison was  $180^\circ-290^\circ$ .

A confidence factor (CF) was provided for each 10 min post processed data by the manufacturer. The definition of this confidence factor is unknown but does have some bearing on data quality. Therefore this parameter was used in the filtering in a purely statistical manner. Data with a CF above or equal to the first quartile were filtered out in order to exclude the main outliers.

In each of the speed regression plots (Figure 42), in addition to the regression parameters, the following fields are also given:

- the wind sector used in the comparison
- the data availability after filtering out the data with the horizontal wind speed of 0.00m/s; the data availability was defined as the ratio between the remaining data and the total number of 10 minute measurements within the wind sector defined above for the period in which this scan was applied (Data avail 1)
- the CF first quartile
- the data availability after filtering out the data with a CF below this threshold (the first quartile); the data availability was defined as the ratio between the remaining data and the number data with a wind speed different from 0.00m/s and within the wind sector defined above (Data avail 2);
- The final number of data after applying all the filtering criteria; the linear regression was applied on the final dataset.
- Data avail 1 shows the ratio of lidar data for which the retrieved horizontal wind speed was different from 0.00m/s.

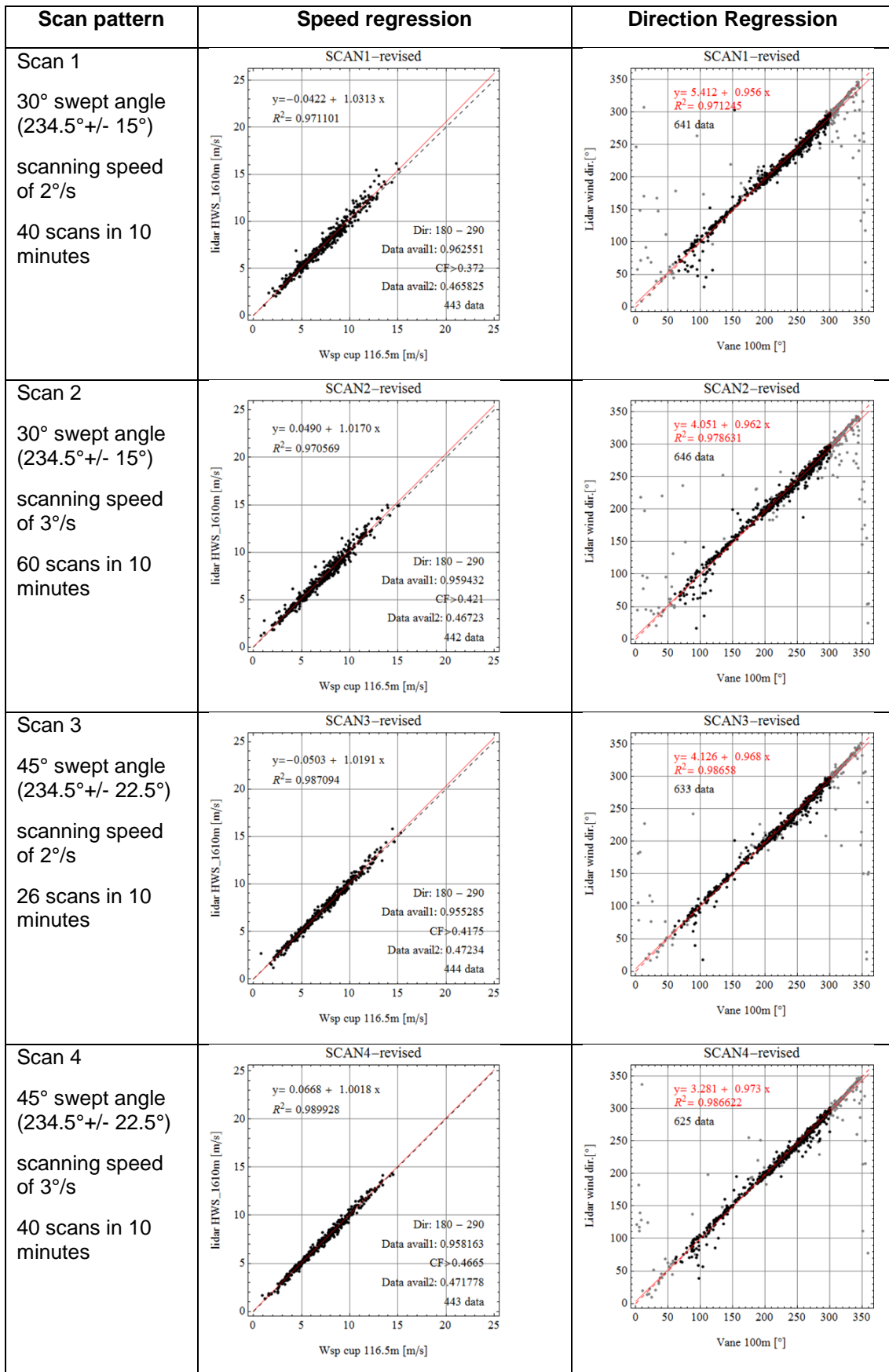


Figure 42 Sector scanning regression results for speed and direction. The linear regression for the wind directions (right panes) are performed only for data (black points) for wind directions between 60 and 300° and wind speeds greater than 3m/s. Direction data falling outside these criteria are shown in grey.

### 3.4.3.2 Error analysis

From the results shown in the previous section for the four different scanning strategies, SCAN4 (45° swept angle and 3°/s scanning speed) has the best overall measurement performance both for wind speed and direction. We have chosen to perform an error analysis with the results from this scanning configuration. In Figure 43, the relative error (lidar horizontal speed/ cup horizontal speed) has been plotted as a function of direction (top panes), wind speed (middle panes) and CF (bottom panes). We have chosen to include the entire dataset in the left panes and the filtered dataset in the right panes. These plots give some insight about how the scatter varies with the different parameters and how effective the filtering has been in removing this scatter.

The upper pane of Figure 43 shows that wind speeds are sensibly valid for the entire range of wind directions. For wind directions roughly perpendicular to the LOS direction (234°), the scatter is significantly larger. Generally excellent wind speed results are obtained in the filtered sector with the lowest scatter for wind speeds coinciding with the LOS direction. The middle panes show that there is no speed related error, as already identified by the gain very close to 1.0.

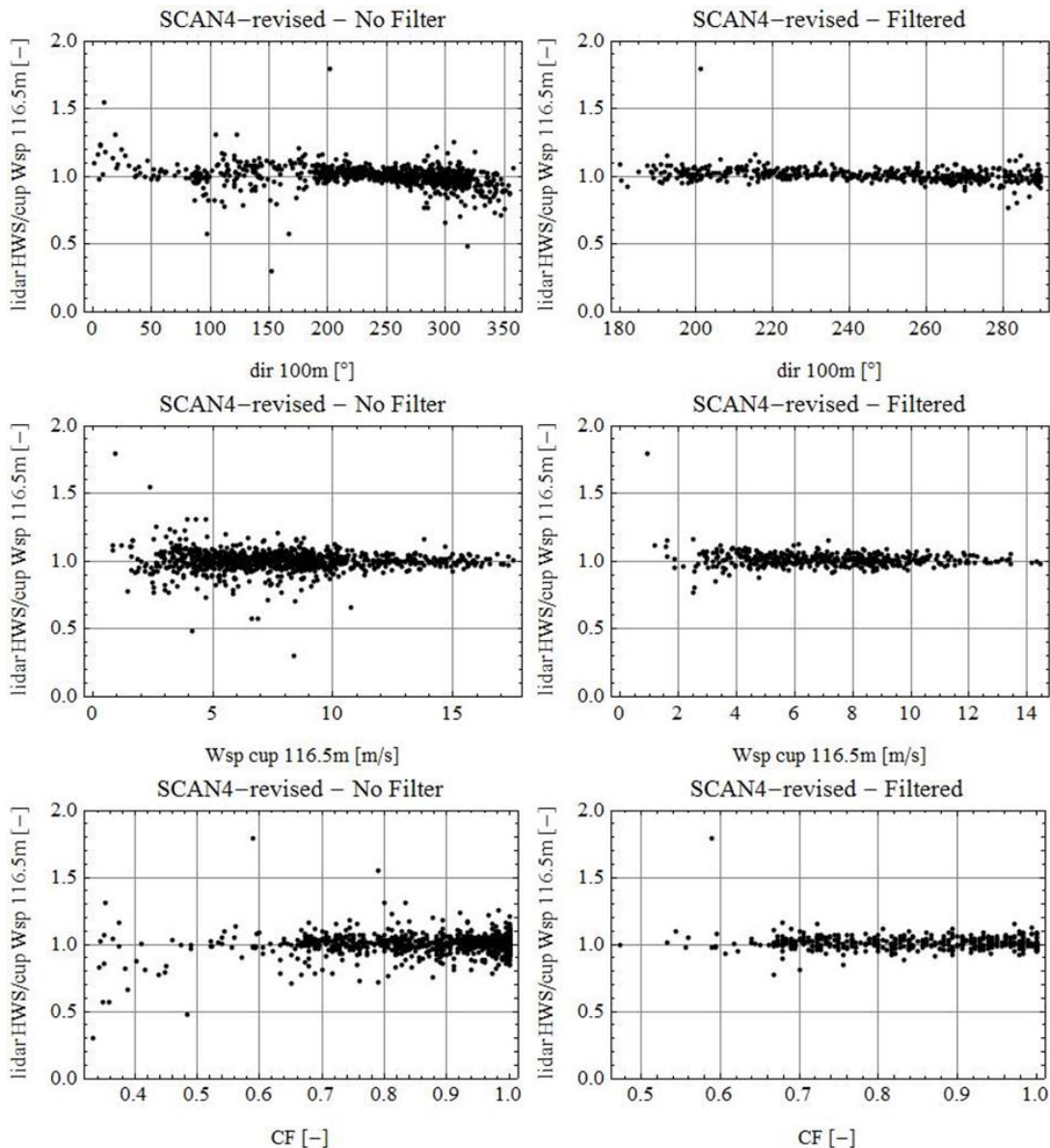




Figure 43 Plots of the lidar to cup wind speed ratio as a function of direction (top), speed (middle) and Confidence Factor (bottom). The left panes are for unfiltered data, the right for filtered data.

### 3.5 SECTOR-SCANNING RESULTS – DISCUSSION

An experiment has been conducted to assess the performance of sector-scanning lidars in a configuration that simulates the measurement of near-shore winds from a coast vantage point. The installation and setup has been described and it has been demonstrated that the angular orientation of lidar remained sensibly constant throughout the duration of the measurement campaign.

The first portion of the campaign was devoted to determining the best scanning strategy in terms of scanning sector width and scanning speed. A wide ( $45^\circ$ ) sector with a fast ( $3^\circ/\text{s}$ ) scanning speed was found to give the best results both for wind speed and direction.

It has been shown that for most wind directions the horizontal wind speed can be reasonably accurately measured, with minimum scatter when the wind direction and LOS directions coincide. For wind directions orthogonal to the sector centreline, the scatter in the wind speed is significantly larger although no systematic bias was observed. When deploying such a system, it would be important to consider how the most common wind directions would be orientated with respect to the sector centreline.

Wind direction could also be reasonably accurately measured, again with the scatter increasing as the wind direction becomes more orthogonal to the sector centreline.

Further work could be carried out to further refine the choice of scanning parameters. It could be advantageous to adapt the scanning pattern according to the relative wind direction or possibly to mix both narrow and wide sectors within a ten minute period in order to best determine both direction and speed.

The uncertainty of a wind resource measurement made with a sector scanning lidar would be largely dominated by the accuracy of the beam elevation angle since this determines the actual measuring height. In this campaign we were measuring at relatively short range (1.5km) and we had a met mast to check the beam elevation. In a real-life measurement the range could be between 5 and 10km and there would be no convenient ‘hard-target’ available to check the beam elevation. Small errors in elevation angle translate to significant sensing height errors at such ranges. Future work must also address the procedures for calibrating elevation angle and correct assessment of the wind speed uncertainties arising from angular uncertainties.

## 4 CONCLUSIONS

This report is the contractual deliverable for the work of Task 4.3.1. Together with internal deliverable D4.16 ([6]) it describes the work carried out in this task.

The work commenced with a thorough survey of the methods available for offshore wind measurements and this is reported in D4.16. A number of various methods are described including conventional measurements on fixed and floating masts, remote sensing from masts and platforms and lastly measurements using floating lidars. Although many of the existing standards and guidelines are at least partially relevant to offshore applications, it is found that there is a need for new recommended practices and international standards, particularly in the area of floating remote sensing systems.

A survey of existing wind datasets was carried out and reported in Section 2 of this document. It is seen that there is a large volume of existing data that have been in particular used to further the understanding of the marine boundary layer. Especially the Fino masts have greatly increased the volume of offshore wind data and provide an important source for research.

As the final contribution to Task 4.3.1, an experiment has been carried out in order to investigate the feasibility of using coastally sited scanning lidars for measuring the wind resource in near-shore areas. This is described in Section 3 of this document. An experiment was performed at a land site where a near-shore measurement campaign was simulated but measuring immediately in the vicinity of a high quality meteorological mast. Various scanning strategies were investigated and it was seen that the best measuring performance was gained by using a fairly wide sector with a fast scanning speed. The achievable measurement performance, both for wind speed and direction is good especially for wind directions approximately aligned to the sector centreline. For wind directions approximately orthogonal to the sector, significantly more scatter is observed although there is no evidence of systematic bias.



## REFERENCES

- [1] Antoniou I., Jørgensen H.E., Mikkelsen T., Frandsen S., Barthelmie R., Perstrup C., and Hurtig M. (2006) Offshore wind profile measurements from remote sensing instruments. Proc. of EWEC, Athens
- [2] Barthelmie R.J., Folkerts L., Larsen G.C., Rados K., Pryor S.C., Frandsen S.T., Lange B., and Shepers G. (2006) Comparison of wake model simulations with offshore wind turbine wake profiles measured by sodar. *J. Atmos. Ocean. Technol.*, 23:888—901
- [3] Barthelmie R.J., Folkerts L., Ormel F.T., Sanderhoff P., Eecen P.J., Stobbe O., and Nielsen M. (2003) Offshore wind turbine wakes measured by sodar. *J. Atmos. Ocean. Technol.*, 20:466—477
- [4] Cañadillas B. and Neumann T. (2012) Sensing the offshore wind in the vicinity of alpha-ventus wind farm: A wind LiDAR study. DEWEK, Bremen
- [5] Cañadillas B., Westerhellweg A., and Neumann T. (2011) Testing the performance of a ground-based wind LiDAR system: one year intercomparison at the offshore platform FINO1. *DEWI Magazine*, 38:58—64
- [6] Courtney M., Peña A., Wagner R., Peeringa J., Brand A., Gottschall J., Rettenmeier A., Pierella F., Giebhardt J. (2013) Report on options for full scale wind resource surveying. Marinet D4.16.
- [7] Xudong Liang (2006) An Integrating Velocity–Azimuth Process Single-Doppler Radar Wind Retrieval Method. *J. Atmos. Ocean. Technol.*, 24:658-665
- [8] Floors R., Vincent C.L., Gryning S.-E., Peña A., and Batchvarova E. (2013) The wind profile in the coastal boundary layer: wind lidar measurements and numerical modeling. *Bound.-Layer Meteorol.*, 147:469—491
- [9] Hasager C.B., Peña A., Mikkelsen T., Courtney M., Antoniou I., Gryning S.-E., Hansen P., and Sørensen P.B. (2007) 12 MW Horns Rev experiment, Tech. Report Risø-R-1506(EN), Risø national Laboratory, Technical University of Denmark, Roskilde
- [10] Hasager C.B., Stein D., Courtney M., Peña A., Mikkelsen T., Stickland M., and Oldroyd A. (2013) Hub height ocean winds over the North Sea observed by the NORSEWIND lidar array: measuring techniques, quality control and data management. *Remote Sens.*, 5:4280—4303
- [11] Kindler D., Oldroyd A., MacAskill A., and Finch D. (2007) An eight month test campaign of the Qinetiq ZephIR system: Preliminary results. *Meteorol. Z.*, 16:479—489
- [12] Mann J., Peña A., Bingöl F., Wagner R., and Courtney M. (2010) Lidar scanning of momentum flux in and above the surface layer. *J. Atmos. Ocean. Technol.*, 27:959—976
- [13] Muñoz-Esparza D., Cañadillas B., Neumann T., and van Beeck J. (2012) Turbulent fluxes, stability and shear in the offshore environment: Mesoscale modeling and field observations at FINO1. *J. Renew. Suist. Energ.*, 4 (063136)
- [14] Peña A. and Gryning S.-E. (2008) Charnock's roughness length model and non-dimensional wind profiles over the sea. *Bound.-Layer Meteorol.*, 128:191—203
- [15] Peña A. and Hahmann A.N. (2012) Atmospheric stability and turbulence fluxes at Horns Rev – and intercomparison of sonic, bulk and WRF model data. *Wind Energy*, 15:717—731

- [16]Peña A. et al. (2013c) Remote sensing for wind energy. DTU Wind Energy-E-Report-0029(EN), DTU Wind Energy, Risø campus, Roskilde
- [17]Peña A., Floors R., and Gryning S.-E. (2013b) The Høvsøre tall wind profile experiment: A description of wind profile observations in the atmospheric boundary layer, in press
- [18]Peña A., Gryning S.-E., and Hahmann A.N. (2013a) Observations of the atmospheric boundary layer height under marine upstream flow conditions at a coastal site. *J. Geophys. Res.*, 118:1924—1940
- [19]Peña A., Gryning S.-E., and Hasager C.B. (2008) Measurements and modelling of the wind speed profile in the marine atmospheric boundary layer. *Bound.-Layer Meteorol.*, 129:479—495
- [20]Peña A., Hasager C.B., Gryning S.-E., Courtney M., Antoniou I., and Mikkelsen T. (2009) Offshore wind profiling using light detection and ranging measurements. *Wind Energy*, 12:105—124
- [21]Peña A., Mikkelsen T., Gryning S.-E., Hasager C.B., Hahmann A.N., Badger M., Karagali I., and Courtney M. (2012) Offshore vertical wind shear: Final report on NORSEWinD's work task 3.1., DTU Wind Energy-E-Report-005(EN), DTU Wind Energy, Risø campus, Roskilde
- [22]Pichugina Y.L., Banta R.M., Brewer W.A., Sandberg S.P., and Hardesty R.M. (2012) Doppler lidar-based wind-profile measurement system for offshore wind-energy and other marine boundary layer applications. *J. Appl. Meteorol. Climatol.*, 51:327—349